Table. Clinical Characteristics of Carriers of A344spl, A341V and "Other" Mutations of Long QT Syndrome

	A344spl	A341V	Others	P value
Genotype-positive, n	31	24	290	
Female sex, n (%)	14 (45)	16 (67)	184 (64)	0.191
Median age-of-onset, years	10±4	9±5	14±14	0.170
Symptomatic, n (%)	13 (42)	14 (58)	98 (34)	0.044
≤15 years of age, n (%)	11 (36)	12 (50)	77 (27)	0.037
<40 years of age, n (%)	12 (39)	14 (58)	90 (31)	0.020
Exercise trigger, n (%*)	11 (85)	13 (93)	66 (67)	0.078
CA/SCD, n (%)	3 (10)	5 (21)	20 (7)	0.053
Heart rate (beats/min)	68±13	67±9	67±12	0.982
QTc, ms	461±30	497±40	474±46	0.011
Corrected QTpeak, ms	389±30	406±23	387±47	0.136
Corrected QTpeak-end, ms	72±17	91±29	86±34	0.044
Schwartz score	3.2±1.7	5.3±2.5	3.2±2.0	<0.001
≥3.5	17 (55)	18 (75)	122 (42)	0.004

*% of symptomatic carriers. CA, cardiac arrest; QTc, corrected QT interval; SCD, sudden cardiac death.

was performed using polymerase chain reaction/single-strand conformation polymorphism or denatured high-performance liquid chromatography analyses and then DNA sequencing in each center.

Clinical Phenotypes in LQT1

The 345 patients in the Japanese cohort were classified as either symptomatic or asymptomatic, based on prior experience of cardiac events (syncope, cardiac arrest (CA), SCD). SCD in a first-degree relative under 40 years old was deemed to be LQTS-related, even in the absence of direct genotyping and/or ECG documentation. Markers of clinical severity were considered to be the proportion of symptomatic mutation carriers, the incidence of life-threatening arrhythmias, age at first cardiac event, and cardiac events before commencing β-blocker therapy, through to 40 years of age. Schwartz scores were also calculated.[19] ECG parameters were measured at baseline, and included RR, QTend (QRS onset to the end of the T-wave interval), QTpeak (QRS onset to the peak of T wave), and QTpeak-end (the peak of T wave to the end of T wave) intervals, as previously described.[12] The QT interval was corrected by Bazett's formula.[20]

Statistical Analysis

Categorical variables are presented as absolute and relative frequencies, and compared using the chi-squared test without Yates continuity correction. Gene variation between each country was compared with Fisher's exact test. Clinical characteristics of genotype groups were compared using Student's t-test as appropriate for continuous variables, which are expressed as the mean and standard deviation. Event-free survival rate was described by Kaplan-Meier cumulative estimates, with comparisons performed by the log-rank test. Time from birth to first event up to 40 years of age was considered for any events, and for CA/SCD. A 2-tailed value of $P < 0.05$ was considered to denote a statistically significant difference. Statistical analysis was performed with SPSS Statistics Version 22 (IBM Corporation, Somers, NY, USA).

Results

Most Common Mutation in the Japanese LQT1 Cohort

Figure 1 shows the distribution of LQT1-related mutations identified at the 3 genetic centers in Japan. Among these, the most frequent was p. A344spl, a splicing mutation involving the substitution of the last base of exon 7 from guanine to adenine (c. 1032 G>A). The A344spl mutation was present in 17 probands (8.9%) in a heterozygous condition.

Typical LQTS Phenotype of A344spl Carriers

In 31 carriers from 17 families with A344spl, the mean age-of-onset was 10±4 years old. A history of cardiac symptoms was present in 13 patients (42%), of whom 11 (36%) had experienced symptoms before 15 years of age; 3 of the 31 carriers (10%) had CA or SCD. Exercise was the major trigger of lethal arrhythmias, being the cause of cardiac events in 11 of the 13 symptomatic patients (85%). The mean corrected QT (QTc) interval in patients with A344spl was 461±30 ms. Using the Schwartz criteria, 17 of 31 patients (55%) had at least 3.5 points, a score that is definitive of LQTS.[19]

Table shows the clinical characteristics of 344 Japanese patients harboring the A344spl (n=31), A341V (n=24), or 'other' (n=290) *KCNQ1* mutations. The missense mutation, A341V, which is located near the A344 codon, is associated with more severe phenotypes,[3] and was the second most common genotype in the present Japanese patients with LQT1 (n=10, **Figure 1**). As previously reported, A341V carriers exhibit severe clinical characteristics, while A344spl carriers are midway in severity between A341V and 'other' mutations, in terms of the mean age-of-onset, symptomatic carriage, frequencies of CA/SCD and Schwartz score of at least 3.5 points. In all groups, the majority of symptomatic carriers had experienced cardiac events during exercise.

Figure 2 shows Kaplan-Meier curves for the cumulative survival to any first cardiac event (syncope, CA, SCD) before the initiation of β-blocker therapy or up to 40 years of age. There was a significant difference among the 3 groups, and approximately 80% of the A341V carriers were symptomatic by the age of 40 years. The prognosis for A344spl carriers was intermediate between that for A341V and 'other' mutation carriers.

Discussion

This multinational study demonstrated that the A344spl *KCNQ1* mutation, which causes a splicing error at exon 7-intron 7,[13,21]

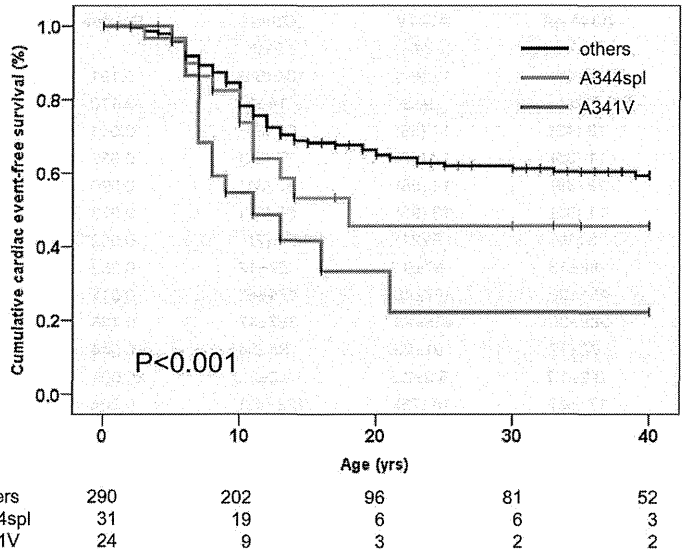

Figure 2. Unadjusted Kaplan-Meier estimates of the cumulative event-free survival in A344spl, A341V, and 'other' mutation carriers among patients with long QT syndrome type 1 (LQT1). Any cardiac event (syncope, cardiac arrest and sudden cardiac death) was considered, from birth up to 40 years of age, and before commencing β-blocker therapy. The A341V mutation was associated with a significantly poorer prognosis than 'other' mutations, and carriers of the A344spl mutation had an intermediate risk of cardiac events.

was common in Japan and the A344spl *KCNQ1* mutation was associated with typical LQTS phenotypes.

KCNQ1 is 1 of 3 major genes responsible for LQTS, and it was revealed by the positional cloning method in 1996.[5] *KCNQ1* encodes the α subunit of the voltage-gated cardiac potassium channel that underlies the slow delayed rectifier potassium current (I_{Ks}). The clinical severity of LQT1 is known to depend on the type and/or location of *KCNQ1* mutations. Moss et al demonstrated that mutations of the transmembrane, missense or dominant-negative type were associated with more severe phenotypes than those of C-terminal, non-missense or haploinsufficiency types.[22] *KCNQ1* mutations in the cytoplasmic loop were reportedly the most severe because modification of the I_{Ks} current by adrenergic stimulation may be impaired.[23] Therefore, variability in *KCNQ1* mutations according to ethnicity or country may affect the outcome of studying clinical phenotypes.

As demonstrated in previous reports, A341V in South Africa,[6,7] Y111C in Sweden[9] and G589D in Finland[10] have been identified as founder mutations with historical data on demographic and clinical characteristics. The A341V mutation is a missense mutation found in South African populations with LQT1, and it is associated with a young age-of-onset, a high frequency of cardiac events, and a longer QTc interval than in non-A341V cohorts. Functional assays also indicated that the A341V phenotype exhibits the dominant-negative effect, with impaired responses to adrenergic stimulation. The Y111C mutation in the N-terminus is frequent in Sweden, and the dominant-negative effect leads to insufficient trafficking of the normal *KCNQ1* protein; however, despite marked QT prolongation, the incidence of cardiac events is lower than for A341V (symptomatic carriers, 30% in Y111C vs. 75% in A341V).[9] In contrast, in Finland, the founder mutation G589D causes a benign phenotype and occurs in 30% of LQTS cases. G589D carriers have mild prolongation of the QT interval (460 ms) under heterozygous conditions, and 26% of patients are symptomatic. These clinical findings are in accordance with an experimental study that confirmed nondominant-negative effects.[10]

The A344spl mutation (c.1032 G>A) was found in all populations, irrespective of country,[24] and may be considered a recurrent mutation. In contrast, the A344spl mutation was significantly more frequent in Japan (8.9%) than in other countries (**Figure 1**: 5 of 160 LQT1, 3.1% in France; 0 of 81 LQT1, 0% in Germany; and 10 of 465 LQT1, 2.1% in the United States;[25] $P<0.05$, $P<0.01$ and $P<0.001$, respectively). Nevertheless, because it was the most frequent mutation in several Japanese genetic centers, it is likely that related cases exist, as for founder mutations.[26] In vitro and in vivo studies demonstrate that A344spl displays various splicing errors, and leads to the dominant-negative pattern.[13] The clinical severity of LQT1 in A344spl carriers was intermediate relative to carriers of A341V and 'other' mutations, which is similar to data from 12 French A344 carriers (clinical characteristics: symptomatic carriers, 42%; mean age-of-onset, 9±5 years; mean QTc, 489±39 ms). The findings of the present study demonstrate that the distribution of common *KCNQ1* mutations differs considerably between countries, and when evaluating clinical data, LQT1 phenotypes associated with hot-spot mutations should be identified.

Conclusions

The A344spl *KCNQ1* mutation was significantly more frequent in Japan than in European countries and the United States. Previous reports have shown the presence of country-specific hot spots in *KCNQ1* mutations, such as A341V in a South African founder population, Y111C in Sweden and G589D in Finland. A344spl carriers demonstrate typical LQTS phenotypes although the clinical severity was intermediate between A341V, associated with malignant phenotypes, and other LQT1 mutations. Thus the severity of *KCNQ1* mutations has been reported to depend on mutation site or type and we should take account of the country when we study the clinical phenotypes of LQT1 corresponding to *KCNQ1* mutations.

Acknowledgments

This work was supported by a Grant-in-Aid for Scientific Research from the Japan Society for the Promotion of Science (JSPS), by a Translational Research Grant from the Japan Circulation Society, by a Grant-in-Aid for Clinical Research on Measures for Intractable Diseases from the Ministry of Health, Labor, and Welfare of Japan (M.H.), a Grant-in-Aid for Scientific Research (C) from JSPS and Grant-in-Aid for Scientific Research on Innovative Areas from The Ministry of Education, Culture, Sports, Science and Technology (MEXT) (H.I.).

Disclosures

None.

References

1. Shimizu W. Update of diagnosis and management of inherited cardiac arrhythmias. *Circ J* 2013; **77:** 2867–2872.
2. Murakoshi N, Aonuma K. Epidemiology of arrhythmias and sudden cardiac death in asia. *Circ J* 2013; **77:** 2419–2431.
3. Mizusawa Y, Horie M, Wilde AA. Genetic and clinical advances in congenital long QT syndrome. *Circ J* 2014; **78:** 2827–2833.
4. Schwartz PJ, Ackerman MJ, George AL, Wilde AA. Impact of genetics on the clinical management of channelopathies. *J Am Coll Cardiol* 2013; **62:** 169–180.
5. Wang Q, Curran ME, Splawski I, Burn TC, Millholland JM, VanRaay TJ, et al. Positional cloning of a novel potassium channel gene: KVLQT1 mutations cause cardiac arrhythmias. *Nat Genet* 1996; **12:** 17–23.
6. Crotti L, Spazzolini C, Schwartz PJ, Shimizu W, Denjoy I, Schulze-Bahr E, et al. The common long-QT syndrome mutation KCNQ1/A341V causes unusually severe clinical manifestations in patients with different ethnic backgrounds: Toward a mutation-specific risk stratification. *Circulation* 2007; **116:** 2366–2375.
7. Brink PA, Schwartz PJ. Of founder populations, long QT syndrome, and destiny. *Heart Rhythm* 2009; **6:** S25–S33.
8. Winbo A, Diamant UB, Stattin EL, Jensen SM, Rydberg A. Low incidence of sudden cardiac death in a Swedish Y111C type 1 long-QT syndrome population. *Circ Cardiovasc Genet* 2009; **2:** 558–564.
9. Winbo A, Diamant UB, Rydberg A, Persson J, Jensen SM, Stattin EL. Origin of the Swedish long QT syndrome Y111C/KCNQ1 founder mutation. *Heart Rhythm* 2011; **8:** 541–547.
10. Piippo K, Swan H, Pasternack M, Chapman H, Paavonen K, Viitasalo M, et al. A founder mutation of the potassium channel KCNQ1 in long QT syndrome: Implications for estimation of disease prevalence and molecular diagnostics. *J Am Coll Cardiol* 2001; **37:** 562–568.
11. Westenskow P, Splawski I, Timothy KW, Keating MT, Sanguinetti MC. Compound mutations: A common cause of severe long-QT syndrome. *Circulation* 2004; **109:** 1834–1841.
12. Itoh H, Shimizu W, Hayashi K, Yamagata K, Sakaguchi T, Ohno S, et al. Long QT syndrome with compound mutations is associated with a more severe phenotype: A Japanese multicenter study. *Heart Rhythm* 2010; **7:** 1411–1418.
13. Tsuji K, Akao M, Ishii TM, Ohno S, Makiyama T, Takenaka K, et al. Mechanistic basis for the pathogenesis of long QT syndrome associated with a common splicing mutation in KCNQ1 gene. *J Mol Cell Cardiol* 2007; **42:** 662–669.
14. Shimizu W, Horie M, Ohno S, Takenaka K, Yamaguchi M, Shimizu M, et al. Mutation site-specific differences in arrhythmic risk and sensitivity to sympathetic stimulation in the LQT1 form of congenital long QT syndrome: Multicenter study in japan. *J Am Coll Cardiol* 2004; **44:** 117–125.
15. Splawski I, Shen J, Timothy KW, Vincent GM, Lehmann MH, Keating MT. Genomic structure of three long QT syndrome genes: KVLQT1, HERG, and KCNE1. *Genomics* 1998; **51:** 86–97.
16. Wang Q, Li Z, Shen J, Keating MT. Genomic organization of the human SCN5A gene encoding the cardiac sodium channel. *Genomics* 1996; **34:** 9–16.
17. Abbott GW, Sesti F, Splawski I, Buck ME, Lehmann MH, Timothy KW, et al. MiRP1 forms IKr potassium channels with HERG and is associated with cardiac arrhythmia. *Cell* 1999; **97:** 175–187.
18. Tristani-Firouzi M, Jensen JL, Donaldson MR, Sansone V, Meola G, Hahn A, et al. Functional and clinical characterization of KCNJ2 mutations associated with LQT7 (Andersen Syndrome). *J Clin Invest* 2002; **110:** 381–388.
19. Schwartz PJ, Crotti L. QTc behavior during exercise and genetic testing for the long-QT syndrome. *Circulation* 2011; **124:** 2181–2184.
20. Bazett HC. An analysis of time relations of the electrocardiograms. *Heart* 1920; **7:** 353–370.
21. Tsuji-Wakisaka K, Akao M, Ishii TM, Ashihara T, Makiyama T, Ohno S, et al. Identification and functional characterization of KCNQ1 mutations around the exon 7-intron 7 junction affecting the splicing process. *Biochim Biophys Acta* 2011; **1812:** 1452–1459.
22. Moss AJ, Shimizu W, Wilde AA, Towbin JA, Zareba W, Robinson JL, et al. Clinical aspects of type-1 long-QT syndrome by location, coding type, and biophysical function of mutations involving the KCNQ1 gene. *Circulation* 2007; **115:** 2481–2489.
23. Barsheshet A, Goldenberg I, O-Uchi J, Moss AJ, Jons C, Shimizu W, et al. Mutations in cytoplasmic loops of the KCNQ1 channel and the risk of life-threatening events: Implications for mutation-specific response to β-blocker therapy in type 1 long-QT syndrome. *Circulation* 2012; **125:** 1988–1996.
24. Murray A, Donger C, Fenske C, Spillman I, Richard P, Dong YB, et al. Splicing mutations in KCNQ1: A mutation hot spot at codon 344 that produces in frame transcripts. *Circulation* 1999; **100:** 1077–1084.
25. Kapplinger JD, Tester DJ, Salisbury BA, Carr JL, Harris-Kerr C, Pollevick GD, et al. Spectrum and prevalence of mutations from the first 2,500 consecutive unrelated patients referred for the familion long QT syndrome genetic test. *Heart Rhythm* 2009; **6:** 1297–1303.
26. Takahashi K, Shimizu W, Miyake A, Nabeshima T, Nakayashiro M, Ganaha H. High prevalence of the SCN5A E1784K mutation in school children with long QT syndrome living on the Okinawa islands. *Circ J* 2014; **78:** 1974–1979.

Heart Vessels
DOI 10.1007/s00380-014-0530-7

CASE REPORT

A high-risk patient with long-QT syndrome with no response to cardioselective beta-blockers

Naoki Toyota · Aya Miyazaki · Heima Sakaguchi · Wataru Shimizu · Hideo Ohuchi

Received: 23 December 2013 / Accepted: 23 May 2014

Abstract We present a case of a high-risk 19-year-old female with long-QT syndrome (LQTS) with compound mutations. She had a history of aborted cardiac arrest and syncope and had received treatment with propranolol for 15 years. However, because she developed adult-onset asthma we tried to switch propranolol, a nonselective beta-blocker, to beta-1-cardioselective agents, bisoprolol and metoprolol. These resulted in both a markedly prolonged corrected QT interval and the development of LQTS-associated arrhythmias. Eventually, propranolol was reinitiated at a higher dose with the addition of verapamil, and she has had no further cardiac or asthmatic events for 5 years.

Keywords Long-QT syndrome · High-risk patient · Beta-blocker · Nonselective beta-blocker · Beta-1 selective blocker

Dr. W Shimizu was supported, in part, by the Research Grant for Cardiovascular Diseases (H24-033) from the Ministry of Health, Labour and Welfare, Japan.

N. Toyota · A. Miyazaki · H. Sakaguchi · H. Ohuchi
Department of Pediatric Cardiology, National Cerebral and Cardiovascular Center, Osaka, Japan

N. Toyota (✉)
Department of Pediatrics, Otsu Red Cross Hospital, 1-1-35 Nagara, Otsu 520-8511, Japan
e-mail: n-toyota@otsu.jrc.or.jp

W. Shimizu
Department of Cardiovascular Medicine, Division of Arrhythmias and Electrophysiology, National Cerebral and Cardiovascular Center, Osaka, Japan

Published online: 11 June 2014

Introduction

The efficacy of beta-blockers in decreasing the incidence of long-QT syndrome (LQTS)-associated cardiac events has been established [1–3]. Although the nonselective beta-blocker, propranolol, is typically used, the relatively cardioselective beta-1-adrenergic agents, bisoprolol and metoprolol, are also used in clinical practice. Recent studies suggest that treatment with metoprolol increases the incidence of cardiac events in symptomatic LQTS when compared with nonselective beta-blockers [4, 5]. However, there is limited evidence regarding the difference in changes induced by beta selectivity in the corrected QT interval (QTc) and serious arrhythmias during rest and exercise in the same patient.

Case report

A 19-year-old female with compound LQT1 mutations (KCNQ1; T322M, H637fs + 28X) was admitted to our hospital for monitoring during a prescription change. She first experienced syncope at the age of 3 years and had been treated with propranolol for LQTS; however, she had a history of aborted cardiac arrest and syncope following a missed dose. Furthermore, she developed asthma at the age of 19 years that required admission to a nearby hospital for treatment. Therefore, it was considered appropriate to switch her treatment from propranolol to a more cardioselective agent (Fig. 1). Although the QTc interval under therapy with propranolol (90 mg/day based on 1.4 mg/kg/day) remained within the normal range, bisoprolol (20 mg/day or 0.3 mg/kg/day) and metoprolol (240 mg/day or 3.7 mg/kg/day) resulted in QTc prolongation (Table 1, Figs. 2, 3). In addition, the treadmill exercise test showed

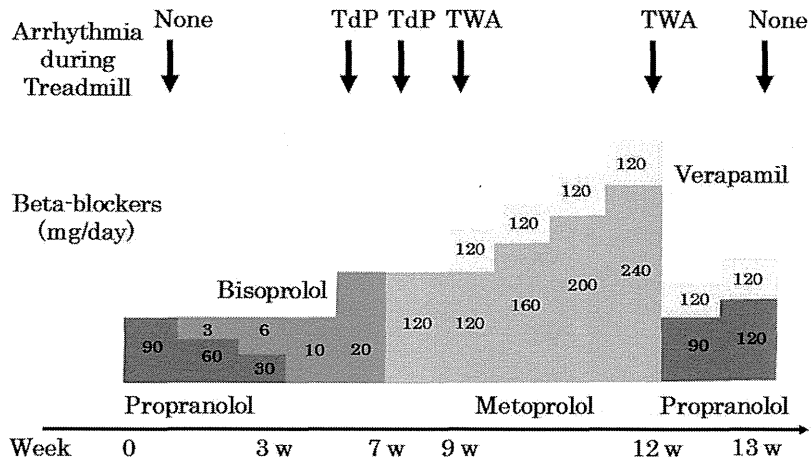

Fig. 1 Transition of beta-blockers and the relationship with corrected QT (QTc) and serious arrhythmias induced by the treadmill exercise test

Table 1 Relationship of beta-blockers and resting heart rate (HR), corrected QT (QTc)

Drug (dose)	Resting HR (bpm)	B-QTc (ms)	F-QTc (ms)
Propranolol (90 mg/day)	63	449	444
Bisoprolol (20 mg/day)	59	495	495
Metoprolol (120 mg/day)	58	463	467
Metoprolol (120 mg/day) + Verapamil (120 mg/day)	65	521	515
Metoprolol (240 mg/day) + Verapamil (120 mg/day)	56	454	458
Propranolol (120 mg/day) + Verapamil (120 mg/day)	56	442	447

B-QTc QT interval corrected for heart rate with Bazett formula, *F-QTc* QT interval corrected for heart rate with Fridericia formula

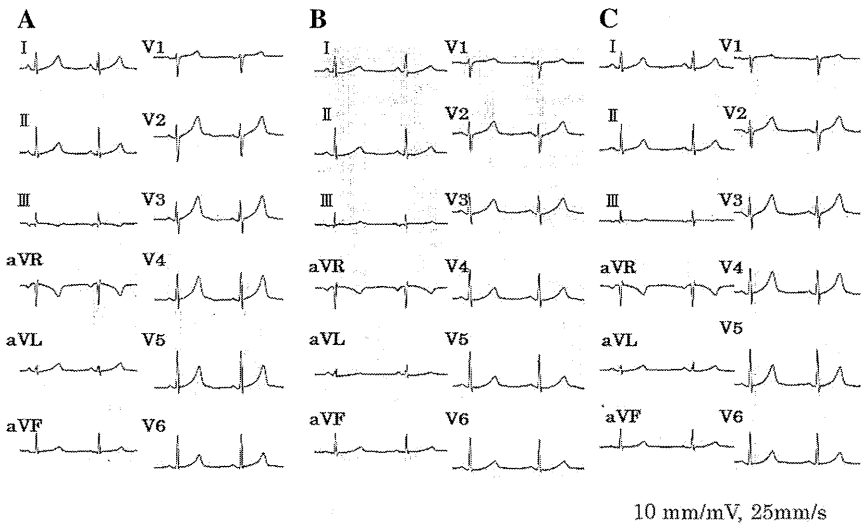

Fig. 2 **a** Surface 12-lead electrocardiogram (ECG) with a heart rate of 63 beats/min (bpm) and a corrected QT (QTc) of 449 ms during therapy with propranolol (90 mg/day or 1.4 mg/kg/day). **b** ECG with a heart rate of 59 bpm and a QTc of 495 ms during treatment with bisoprolol (20 mg/day or 0.3 mg/kg/day). **c** ECG with a heart rate of 59 bpm and a QTc of 455 ms during treatment with metoprolol (240 mg/day or 3.7 mg/kg/day) and verapamil (120 mg/day or 1.6 mg/kg/day)

her attenuated QT shortening and exaggerated QTc prolongation, which induced T-wave alternans and torsade de pointes (Figs. 4, 5). We determined that metoprolol and bisoprolol were ineffective against LQTS-associated cardiac events in this patient and eventually opted to continue propranolol at an increased dose of 120 mg/day (1.8 mg/kg/day) in addition to verapamil (120 mg/day or 1.8 mg/kg/day) with the consent of the patient and her parents. Since then, she has suffered from no cardiac or asthmatic events for 5 years.

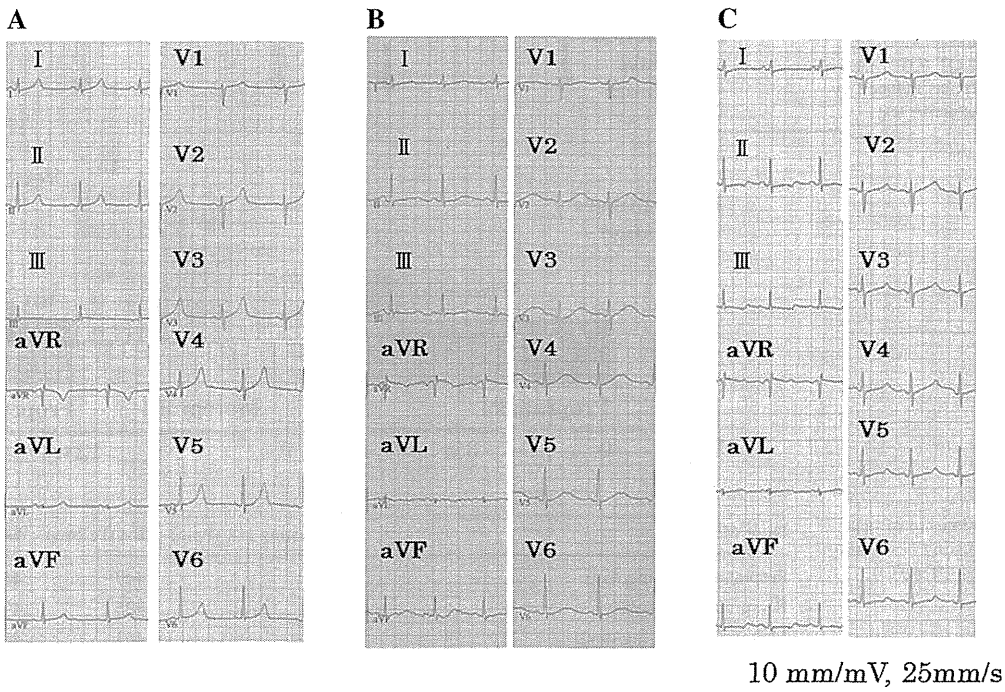

Fig. 3 **a** Surface 12-lead electrocardiogram (ECG) at rest just before treadmill exercise test with a heart rate of 63 beats/min (bpm) and a corrected QT (QTc) of 444 ms during therapy with propranolol (90 mg/day or 1.4 mg/kg/day). **b** ECG at rest just before treadmill with a heart rate of 77 bpm and a QTc of 688 ms during treatment with bisoprolol (20 mg/day or 0.3 mg/kg/day). **c** ECG at rest just before treadmill with a heart rate of 85 bpm and QTc of 597 ms during treatment with metoprolol (240 mg/day or 3.7 mg/kg/day) and verapamil (120 mg/day or 1.6 mg/kg/day)

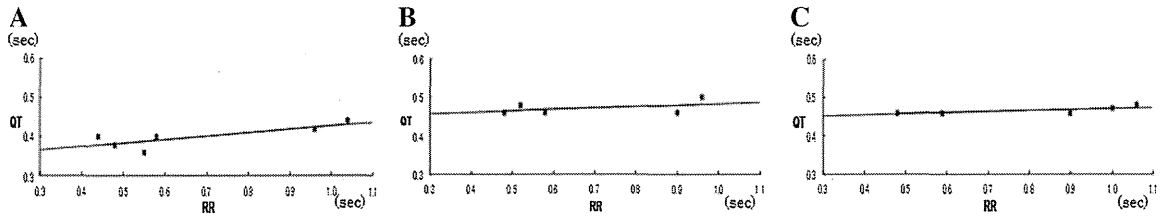

Fig. 4 Relation of QT to R–R intervals during exercise. *Solid lines* are best fit by least-squares method. Slope of each line (QT/R–R) was 0.08, 0.04, and 0.03, respectively. **a** Relation of QT to R–R intervals during exercise during treatment with propranolol (90 mg/day or 1.4 mg/kg/day). **b** Relation of QT to R–R intervals during exercise during treatment with bisoprolol (20 mg/day or 0.3 mg/kg/day). **c** Relation of QT to R–R intervals during exercise during treatment with metoprolol (240 mg/day or 3.7 mg/kg/day) and verapamil (120 mg/day or 1.6 mg/kg/day)

Discussion

Congenital long-QT syndrome is an inherited channelopathy, characterized by prolonged and abnormal repolarization and associated with a high risk of ventricular arrhythmias, syncope, seizures, and sudden death [3, 6, 7]. To date, at least 12 LQTS genotypes have been identified, of which LQTS variants 1–3 account for approximately 90 % identified cases [7]. Moreover, recent molecular developments have enabled us to understand genotype–phenotype correlations and gene-specific arrhythmic triggers [8]. Compound mutation carriage is associated with a more severe phenotype than is observed with single mutation carriage [9, 10].

The efficacy of beta-blockers in decreasing the incidence of LQTS-associated cardiac events has been established [1, 2], and beta-blockers are first-line options for LQTS variants 1 and 2 [2]. However, approximately 15–30 % treated patients continue to experience breakthrough cardiac events despite beta-blocker treatments [1,

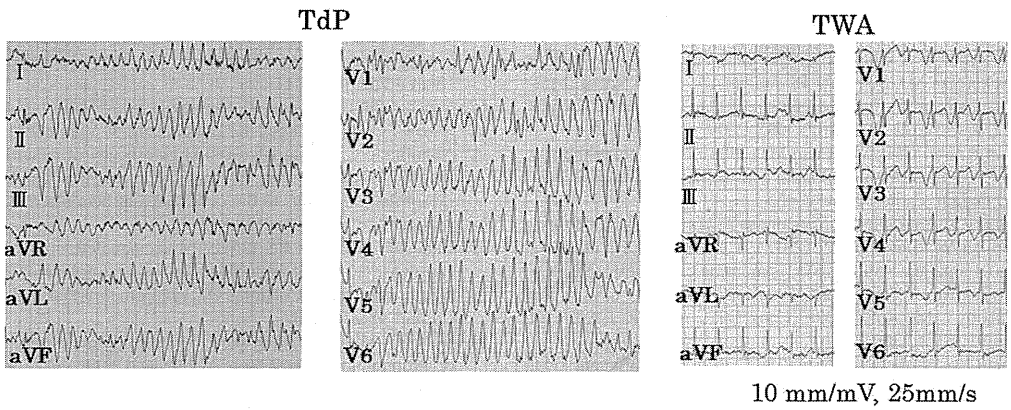

Fig. 5 The treadmill exercise test induced typical torsade de pointes (TdP; *left panel*) and T-wave alternans (TWA; *right panel*). TdP under bisoprolol (20 mg/day or 0.3 mg/kg/day). TWA under metoprolol (240 mg/day or 3.7 mg/kg/day) and verapamil (120 mg/day or 1.6 mg/kg/day)

4, 11, 12]. In fact, recent studies have suggested that not all beta-blockers are equal in their antiarrhythmic efficacy [4, 5]. Chatrath and colleagues [5] concluded that treatment with atenolol, young age at diagnosis, and noncompliance are important factors underlying beta-blocker treatment failure. Chockalingam and colleagues [4] recommended that symptomatic LQTS (variants 1 and 2) are treated with either propranolol or nadolol, while metoprolol should not be used. Although propranolol and nadolol are nonselective beta-blockers, atenolol and metoprolol are relatively cardioselective beta-1-blockers.

Although the mechanism underlying different treatment outcomes remains unclear, the efficacy of cardiac sodium-channel blocking may be an important factor. A recent study has demonstrated that the sodium-channel blocking effect of propranolol is particularly marked on the late noninactivating sodium-ion current than on the peak sodium-ion current, which is not observed with metoprolol [13, 14]. Although it has been observed that bisoprolol decreased QT dispersion in chronic heart failure [15], there is limited data available on bisoprolol for LQTS patients with normal heart structure [3, 16]. Nonetheless, bisoprolol is discouraged because it is also a beta-1-selective blocker such as metoprolol and may lack the sodium-channel blocking effect of propranolol.

Some reports discussed the effects of beta-blocker therapy on ventricular repolarization. Chockalingam and colleagues [4] reported that propranolol had a significantly better QTc shortening effect as compared to metoprolol and nadolol, especially in LQT1/LQT2 patients with prolonged QTc. On the other hand, Extramina and colleagues [17] reported that beta-blocker treatment was associated with a significant prolongation of the QT interval in LQT1 patients whereas it shortened the QT interval in LQT2 patients. Moss and colleagues [1] reported only minimal change in QTc in their LQT1/LQT2 patients with beta-blocker therapy. These differences may reflect the difference of severity of illness in study population, the influence of rate correction, or variation of beta-blockers. We could not evaluate the change of QT interval based on presence or absence of beta-blocker. However, propranolol appeared to improve QT shortening at upper heart rate somewhat better than bisoprolol and metoprolol (Fig. 4).

The patient in this report was classified as high-risk [2, 3, 9, 18]. Consistent with earlier reports, beta-1-selective blockers could not suppress potentially lethal arrhythmias. Therefore, we recommend the use of nonselective beta-blockers for patients with symptomatic high-risk LQTS. If nonselective beta-blockers are contraindicated, additional treatment may be necessary. Options include an implantable cardioverter defibrillator (ICD) and left cervical sympathetic denervation [2, 18].

References

1. Moss AJ, Zareba W, Hall WJ, Schwartz PJ, Crampton RS, Benhorin J, Vincent GM, Locati EH, Priori SG, Napolitano C, Medina A, Zhang L, Robinson JL, Timothy K, Towbin JA, Andrews ML (2000) Effectiveness and limitations of beta-blocker therapy in congenital long-QT syndrome. Circulation 101:616–623
2. Goldenberg I, Bradley J, Moss A, Mcnitt S, Polonsky S, Robinson JL, Andrewa M, Zareba W (2010) Beta-blocker efficacy in high-risk patients with the congenital long-QT syndrome types 1 and 2: implications for patient management. J Cardiovasc Electrophysiol 21:893–901
3. Goldenberg I, Moss AJ, Peterson DR, McNitt S, Zareba W, Andrews ML, Robinson JL, Locati EH, Ackerman MJ, Benhorin J, Kaufman ES, Napolitano C, Priori SG, Qi M, Schwartz PJ, Towbin JA, Vincent GM, Zhang L (2008) Risk factors for aborted cardiac arrest and sudden cardiac death in children with the congenital long-QT syndrome. Circulation 117:2184–2191

4. Chockalingam P, Crotti L, Girardengo G, Johnson JN, Harris KM, Heijden JF, Hauer RN, Beckmann BM, Spazzolini C, Rordorf R, Rydberg A, Clur SA, Fischer M, Heuvel F, Kaab S, Blom NA, Ackerman MJ, Schwartz PJ, Wilde AA (2012) Not all beta-blockers are equal in the management of long QT syndrome types 1 and 2. J Am Coll Cardiol 60:2092–2099
5. Chatrath R, Bell CM, Ackerman MJ (2004) Beta-blocker therapy failures in symptomatic probands with genotyped long-QT syndrome. Pediatr Cardiol 25:459–465
6. Nakashima K, Kusakawa I, Yamamoto T, Hirabayashi S, Hosoya R, Shimizu W, Sumitomo N (2013) A left ventricular noncompaction in a patient with long QT syndrome caused by a KCNQ1 mutation: a case report. Heart Vessels 28:126–129
7. Goldenberg I, Moss AJ (2008) Long QT syndrome. J Am Coll Cardiol 51:2291–2300
8. Schwartz PJ, Priori SG, Spazzolini C, Moss AJ, Vincent GM, Napolitano C, Denjoy I, Guicheney P, Breithardt G, Keating MT, Towbin JA, Beggs AH, Brink P, Wilde AA, Toivonen L, Zareba W, Robinson JL, Timothy KW, Corfield V, Wattanasirichaigoon D, Corbett C, Haverkamp W, Schulze-Bahr E, Lehmann MH, Schwartz K, Coumel P, Bloise R (2001) Genotype–phenotype correlation in the long-QT syndrome: gene-specific triggers for life-threatening arrhythmias. Circulation 103:89–95
9. Itoh H, Shimizu W, Hayashi K, Yamagata K, Sakaguchi T, Ohno S, Makiyama T, Akao M, Ai T, Noda T, Miyazaki A, Miyamoto Y, Yamagishi M, Kamakura S, Horie M (2010) Long QT syndrome with compound mutations is associated with a more severe phenotype: a Japanese multicenter study. Heart Rhythm 7:1411–1418
10. Bando S, Soeki T, Matsuura T, Niki T, Ise T, Yamaguchi K, Taketani Y, Iwase T, Yamada H, Wakatsuki T, Akaike M, Aiba T, Shimizu W, Sata M (2013) Congenital long QT syndrome with compound mutations in the KCNH2 gene. Heart Vessels. doi: 10.1007/s00380-013-0406-2
11. Villain E, Denjoy I, Lupoglazoff JM, Guicheney P, Hainque B, Lucet V, Bonnet D (2004) Low incidence of cardiac events with beta-blocking therapy in children with long QT syndrome. Eur Heart J 25:1405–1411
12. Vincent GM, Schwartz PJ, Denjoy I, Swan H, Bithell C, Spazzolini C, Crotti L, Piippo K, Lupoglazoff J, Villain E, Priori SG, Napolitano C, Zhang L (2009) High efficacy of beta-blockers in long-QT syndrome type 1: contribution of noncompliance and QT-prolonging drugs to the occurrence of beta-blocker treatment "failures". Circulation 119:215–221
13. Bankston JR, Kass RS (2010) Molecular determinants of local anesthetic action of beta-blocking drugs: implication for therapeutic management of long QT syndrome variant 3. J Mol Cell Cardiol 48:246–253
14. Duff HJ, Mitchell LB, Wyse DG (1986) Antiarrhythmic efficacy of propranolol: comparison of low and high serum concentrations. J Am Coll Cardiol 8:959–965
15. Aygul N, Ozdemir K, Duzenli MA, Aygul MU (2009) The comparative effects of long-term carvedilol versus bisoprolol therapy on QT dispersion in patients with chronic heart failure. Cardiology 112:168–173
16. Viitasalo M, Oikarinen L, Swan H, Vaananen H, Jarvenpaa J, Hietanen H, Karjalainen J, Toivonen L (2006) Effects of beta-blocker therapy on ventricular repolarization documented by 24-h electrocardiography in patients with type 1 long-QT syndrome. J Am Coll Cardiol 48:747–753
17. Extramiana F, Maison-Blanche P, Denjoy I, Jode PD, Messali A, Labbe JP, Leenhardt A (2013) Gene-specific effect of beta-adrenergic blockade on corrected QT interval in the long QT syndrome. Ann Noninvasive Electrocardiol 18:399–408
18. Jons C, Moss AJ, Goldenberg I, Liu J, McNitt S, Zareba W, Qi M, Robinson JL (2010) Risk of fatal arrhythmic events in long QT syndrome patients after syncope. J Am Coll Cardiol 55:783–788

Acetylcholine Suppresses Ventricular Arrhythmias and Improves Conduction and Connexin-43 Properties During Myocardial Ischemia in Isolated Rabbit Hearts

TAKESHI AIBA, M.D., PH.D.,* TAKASHI NODA, M.D., PH.D.,* ICHIRO HIDAKA, M.S.,† MASASHI INAGAKI, M.D.,† RAJESH G. KATARE, M.D.,‡ MOTONORI ANDO, PH.D.,‡ KENJI SUNAGAWA, M.D., PH.D.,§ TAKAYUKI SATO, M.D., PH.D.,‡ and MASARU SUGIMACHI, M.D., PH.D.†

From the *Division of Arrhythmia and Electrophysiology, Department of Cardiovascular Medicine; †Department of Cardiovascular Dynamics, Research Institute, National Cerebral and Cardiovascular Center Suita, Japan; ‡Department of Cardiovascular Control, Kochi Medical School, Nankoku, Japan; and §Department of Cardiovascular Medicine, Kyushu University Graduate School of Medical Sciences, Fukuoka, Japan

ACh Prevents Ischemic Loss of Gj and Arrhythmias. ***Introduction:*** **Acetylcholine (ACh), a vagal efferent neurotransmitter, markedly improves survival in rats with myocardial ischemia (MI) by preventing ischemic loss of gap junction (Gj) and by inducing anti-apoptotic cascades. However, electrophysiological mechanisms of the antiarrhythmic effect of ACh after acute MI are still unclear.**

Methods: **Acute MI was induced by ligation of the left anterior descending (LAD) coronary artery in Langendorff-perfused rabbit hearts with (ACh(+):n = 11) or without (ACh(–):n = 12) 10 μmol/L ACh delivered continuously starting at 5 minutes before LAD ligation. Action potentials on the left ventricular (LV) anterior surface (≈2×2 cm) were recorded by optical mapping during pacing from the LV epicardium (BCL = 500 milliseconds). Conduction velocities (CVs) at 256 sites were calculated and the ventricular tachycardia/ventricular fibrillation (VT/VF) susceptibility was also assessed by programmed electrical stimulation before and 30 minutes after MI. The amount and distribution of Gj protein connexin-43 was analyzed by immunoblotting and immunohistochemistry.**

Results: **Averaged CV in the ischemic border zone (IBZ) was significantly slower in ACh(–) than in ACh(+) (21 ± 7 vs. 34 ± 6 cm/s; P < 0.01). Short-coupled extra stimulus further decreased CV of IBZ in ACh(–) (13 ± 4 cm/s) but did not change that in ACh(+) (34 ± 5 cm/s), leading to a high incidence of conduction block in IBZ in ACh(–) but not in ACh(+) (83% vs. 0%). VT/VF after MI were induced in ACh(–) but suppressed in ACh(+) (10/12 vs. 3/11; P < 0.01). Connexin-43 in the LV anterior wall was significantly reduced after MI in ACh(–) but not in ACh(+).**

Conclusion: **ACh may suppress VT/VF by preventing loss of Gj and improving CV in IBZ during acute MI.** *(J Cardiovasc Electrophysiol, Vol. 26, pp. 678-685, June 2015)*

acetylcholine, conduction, connexin-43, gap junction, ischemia, optical mapping, ventricular arrhythmias

Introduction

Ventricular tachycardia or ventricular fibrillation (VT/VF) after acute myocardial ischemia (MI) play critical roles in sudden cardiac death in humans.[1] The first clinical manifestation of patients with acute MI is often VT/VF or sudden cardiac death. Previous clinical trials with antiarrhythmic drugs have failed to reduce the incidence of sudden cardiac death and even increased mortality in the treated group.[2] Acute MI markedly reduces tissue pH,[3] increases the interstitial potassium and intracellular calcium levels,[4] and causes neurohumoral changes,[5] all of which contribute to the development of electrical instability that lead to VT/VF. The gap junction protein connexin-43 (Cx43) is considered to play an essential role in the propagation of cardiac electrical impulses.[6] Slow conduction caused by reduced gap junction in the ischemic border zone (IBZ) results in a potent arrhythmogenic substrate after acute MI.[7-14]

Decreased cardiac parasympathetic control in a setting of abnormally augmented sympathetic drive during acute MI increases the risk of sudden cardiac death as a result of VT/VF.[15] We previously reported that acetylcholine (ACh), a vagal efferent neurotransmitter, markedly improved survival in rats with MI by preventing ischemic loss of gap junction and by inducing anti-apoptotic cascades.[16-19] Vagal nerve stimulation prevented cesium-induced early after depolarization,[20] and suppressed VT/VF in dog models of

This study was supported by the Japan Science and Technology Agency and a Health and Labour Sciences Research grant for research on medical devices for analyzing, supporting, and substituting the function of the human body and by Health and Labor Sciences Research Grants (H20-katsudo-Shitei-007 and H21-trans-Ippan-013) from the Ministry of Health, Labor and Welfare of Japan.

Disclosures: None.

Address for correspondence: Takeshi Aiba, M.D., Ph.D., Division of Arrhythmia and Electrophysiology, Department of Cardiovascular Medicine, National Cerebral and Cardiovascular Center, Suita, Japan, 5-7-1 Fujishiro-dai, Suita, Osaka 565-8565 Japan. Fax: 81-6-6872-7486; E-mail: aiba@hsp.ncvc.go.jp

Manuscript received 18 January 2011; De novo manuscript received 9 February 2015; Accepted for publication 25 February 2015.

doi: 10.1111/jce.12663

acute[21] and chronic MI[22] as well as anesthetized cats with acute MI[23] and conscious rats with heart failure.[24] These findings suggest that increased cardiac vagal tone may reduce the risk of sudden arrhythmic death. Nevertheless, the detailed electrophysiological mechanisms of the antiarrhythmic effect of ACh remain unclear. In this study, we test the hypothesis that ACh suppresses VT/VF by preventing loss of gap junction during acute MI and improving the conduction velocity (CV) in the IBZ. Using a novel high-resolution optical mapping of action potential (AP) with a freely beating heart, we first characterized how ACh altered the CV in the IBZ and VT/VF susceptibility during acute MI in Langendorf-perfused isolated rabbit hearts, which will aid in the identification of a new therapeutic strategy to prevent sudden cardiac death during acute MI.

Methods

Preparation and Study Protocol

All animal care procedures conformed to the standards of the American Heart Association regarding the use of animals in research (November 11, 1984). All protocols were approved by the Animal Subjects Committee of the National Cerebral and Cardiovascular Center of Japan. Adult male Japanese white rabbits (2.5–3.5 kg) were anesthetized by intravenous injection of sodium pentobarbital (35 mg/kg). Hearts were isolated and perfused as Langendorff preparations with Tyrode's solution of the following compositions (in mmol/L): 129 NaCl, 4 KCl, 0.9 NaH_2PO_4, 20 $NaHCO_3$, 1.8 $CaCl_2$, 0.5 $MgSO_4$, and 5.5 glucose, buffered with 95% O_2 and 5% CO_2. The temperature was maintained at 35 ± 1 °C and perfusion pressure was maintained at 80 mmHg. The right atrium was removed to avoid competitive stimulation from the sinoatrial node.

Left ventricular (LV) epicardial pacing at a basic cycle length (BCL) of 500 milliseconds was performed using a unipolar electrode attached to the center of the anterior wall. An electrocardiograph (ECG) was recorded by electrodes attached to the right and left ventricular epicardium, ground to the aortic root. After staining with dye, di-4-ANEPPS (10 μmol/L; Molecular Probes Inc.), acute MI was created by ligating the left anterior descending coronary artery with (ACh(+): n = 11) or without (ACh(–): n = 12) 10 μmol/L ACh. In ACh(+) heart, ACh treatment was initiated 5 minutes before coronary ligation.

Optical Action Potential Mapping in Freely Beating Rabbit Heart

We recorded the fluorescence of di-4-ANEPPS using dual complementary metal–oxide–semiconductor (C-MOS) sensors, as described previously.[25-27] In brief, after staining with a voltage-sensitive dye, di-4-ANEPPS (10 μmol/L; Molecular Probes Inc.), excitation of the dye's fluorescence was achieved with 480 ± 15 nm light through a bandpass filter (ANDV8247, Andover, Salem, NH) from a bluish-green emission diode (E1L51-3B0A4-02, Toyoda Gosei, Aichi, Japan). The optical recording was centered 5 mm lateral to the left anterior descending coronary artery, halfway between the base and the apex, and covered a ≈19.3 × 19.3 mm area of the left ventricular anterior epicardium (spatial and temporal resolution of 60–70 μm and 2 milliseconds).

Fluorescent light from the heart was split using a dichroic mirror and narrowed down to 2 frequency bands (≈540 or 690 nm) through a bandpass filter (ANDV8368 or ANDV7845, respectively). Next, the dual-wavelength lights were simultaneously focused onto 10-bit 256×256 element dual C-MOS sensors (Hamamatsu Photonics, Hamamatsu, Japan) using image intensifiers (FASTCAM-Ultima, Photron, Tokyo, Japan) at 500 frames/s. Both signals were stored on the hard disk of a dedicated laboratory computer system, and analyzed using our laboratory's original software.

Contraction artifacts of AP were eliminated with motion tracking and ratiometry of both signals. We placed several small beads (0.5 mm ϕ) on the epicardial surface as landmarks (Supporting Fig. S1A), which were automatically tracked by computer software during optical recording (Supporting Fig. S1B). Next, D(t), the displacement vector of the observatory point at frame t, was predicted by the weighted sum of the displacement vectors of the markers using the following equation (Supporting Fig. S1C) (1):

$$D(t) = \sum_{i=1}^{n} k_i d_i(t). \quad (1)$$

The weighted coefficient k_i was determined by the distance between marker i and the observatory point, l_i, as equation (2):

$$k_i = \frac{\exp(-l_i/\tau)}{\sum_{m=1}^{n} \exp(-l_m/\tau)} \quad (2)$$

where τ = (averaged distance between markers) × 0.5.

After modification of the optical signals by tracking, ratiometry of both signals can be used to further subtract a motion artifact, as described previously. Then, the voltage of the optical signal recorded at each site was automatically displayed in color (lowest: black; highest: red) and plotted in the 256 × 256 matrix as an isopotential map. Transmembrane action potentials (APs) from 256 sites (16 × 16 units) on the left ventricular (LV) epicardial surface were displayed.

Electrophysiological Study

To assess the VT/VF susceptibility, we performed a single extra stimulus (S2) delivered after every 10th basic beat (S1) paced from the epicardial surface at a BCL of 500 milliseconds as a 10 milliseconds decremental step interval until the effective refractory period before (baseline) and 30 minutes after MI with or without ACh. CV and action potential duration at 75% of repolarization (APD_{75}) at 256 LV sites at the programmed electrical stimuli (PES) were calculated by optical mapping data.

Ischemic and Ischemic Border Zone

The ischemic zone (IZ) was defined as the area in which the AP amplitude was decreased over 80% after 30 minutes of LAD ligation compared to baseline. The ischemic border zone (IBZ) was defined as portions with a 5 mm margin from the IZ. The remaining area was defined as the nonischemic zone (NIZ) (Fig. 1B, C). To confirm the area of lower AP-amplitudes as an ischemic zone, triphenyltetrazolium chloride (TTC) staining was performed in some isolated rabbit hearts and the electrophysiological ischemic area was

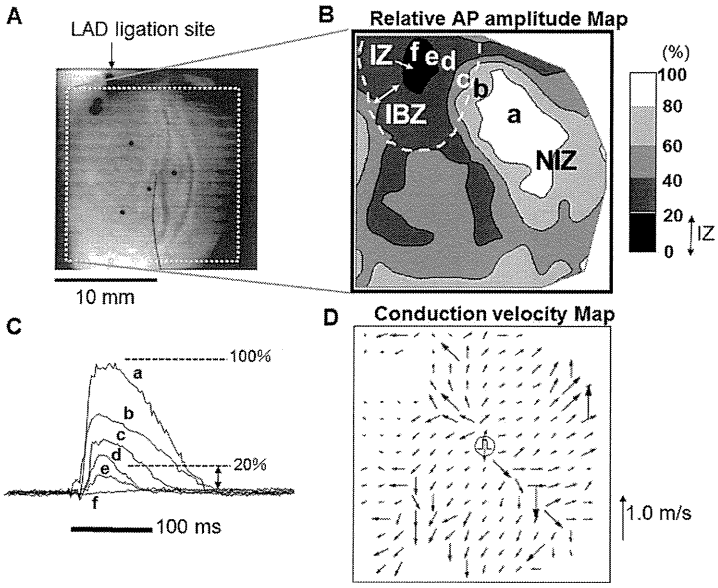

Figure 1. *Distributions of action potential amplitude and conduction velocity after acute MI. A: Optical photo shows the ligation site of the left anterior descending coronary artery (LAD) and the area (dotted square) capable of recording the optical action potential (AP) signals. B, C: Distribution of changes (%) in AP amplitude before (baseline) and 30 minutes after MI and superimposed APs at each site (a–f) of the LV surface. The ischemic zone (IZ) was defined as the area where AP amplitude after MI decreased by over 80% of the baseline level (black). The ischemic border zone (IBZ) was defined as portions with a 5 mm margin from the ischemic zone and the remaining area was defined as the nonischemic zone (NIZ). D: Conduction velocity (CV) map paced from the LV anterior surface (center of the map) shows that the CV was significantly slower in the IBZ compared with the NIZ.*

almost consistent with histological infarct areas (Supporting Fig. S2).

Immunoblotting and Immunohistochemistry

The amount and distribution of gap junction protein Cx43 were analyzed by Western immunoblotting and immunohistochemistry, as previously described.[17] Detailed methods are provided in the online supporting data.

Statistical Analysis

Differences between multiple groups were compared by an analysis of variance (ANOVA) followed by an appropriate multiple comparison test. Two-group analysis was performed by a *t*-test (paired or unpaired as appropriate). Serial studies were tested by repeated measures ANOVA. Data were expressed as mean values ± SD except for those shown in the figures, which were expressed as mean ± SEM. A value of $P < 0.05$ was considered significant.

Results

Effect of Acetylcholine on Excitation Propagation

Representative optical isochronal activation maps are depicted in Figure 2A–C. In the baseline (Fig. 2A), the isochronal activation map illustrates the normal anisotropic conduction pattern from the pacing site. Acute MI, however, prolonged the activation time in the IBZ, especially during the shorter S1–S2 intervals (Fig. 2B). However, ACh prevented the MI-induced prolongation of activation time in the IBZ not only at the BCL but also at the shorter coupling interval (Fig. 3C). Figure 2D–F summarizes the relationship between the pacing coupling interval and the averaged CV at the baseline (Fig. 2D) and after MI in the absence (Fig. 2E) or presence of ACh (Fig. 2F). Even after MI, the averaged CV in the NIZ in the absence or presence of ACh was the same as that of the baseline (42 ± 9, 42 ± 7 vs. 42 ± 6 cm/s, respectively, at the BCL of 500 milliseconds). However, the averaged CV in the IBZ after MI was significantly lower than the baseline (21 ± 7 vs. 42 ± 6 cm/s at the BCL of 500 milliseconds; $P < 0.01$), whereas the CV in the IBZ in the presence of ACh (MI+ACh) was not significantly decreased in spite of ischemia (34 ± 6 cm/s, P = NS vs. baseline). Most notably, the averaged CV was significantly decreased at the shorter coupling interval (150 milliseconds) compared with that at the BCL of 500 milliseconds in the baseline (33 ± 8 vs. 42 ± 6 cm/s; $P < 0.05$) and after MI (NIZ: 30 ± 9 vs. 42 ± 9 cm/s; $P < 0.05$, and IBZ: 13 ± 4 vs. 21 ± 7 cm/s; $P < 0.05$) but it was not decreased in MI+ACh even at the shorter coupling interval (NIZ: 40 ± 9 vs. 42 ± 7 cm/s; P = NS, and IBZ: 34 ± 5 vs. 34 ± 6 cm/s; P = NS). Thus, ACh prevented MI-induced conduction delay in the IBZ.

Effect of Acetylcholine on Repolarization

Table 1 summarizes the effect of ACh on repolarization parameters. Ischemia significantly abbreviated the minimum but not the maximum APD_{75} in the LV anterior epicardial surface, resulting in significant abbreviation of the averaged APD_{75} in MI compared to the baseline. However, these MI-induced changes of the repolarization parameters were not restored by ACh. Moreover, the effective refractory period was not significantly different between the baseline and after MI with or without ACh. Therefore, ACh did not affect repolarization parameters after acute MI.

VT/VF Susceptibility

The shorter S1–S2 interval by PES from the LV anterior epicardium highly induced uni-directional conduction block in the IBZ after MI (Fig. 3A), whereas PES did not induce conduction block in MI + ACh (83% vs. 0%). Neither VT nor VF was induced by PES in the baseline, whereas VF was highly (83%) induced by PES after acute MI but was rare (27%) or spontaneously terminated in MI + ACh (Fig. 3B). Figure 3C and 3D summarize the frequency of nonsustained VT (terminated within 15 s) and sustained VT or VF induced by PES after MI in the absence or presence of ACh, demonstrating that ACh strongly suppressed the PES-induced nonsustained or sustained VT/VF after acute MI.

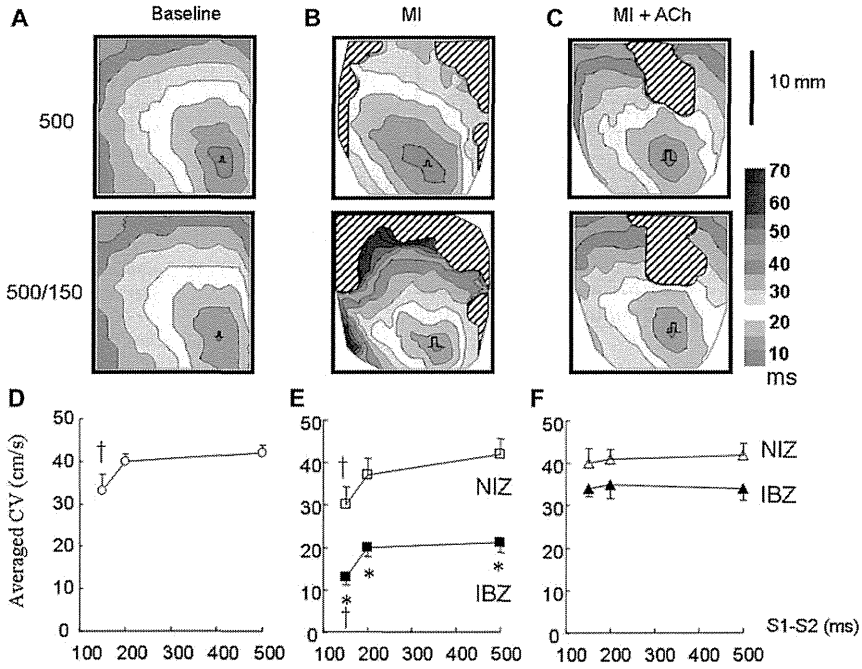

Figure 2. *Optical isochronal activation map and averaged conduction velocity (CV) in the baseline, nonischemic zone (NIZ) and ischemic border zone (IBZ) after myocardial ischemia in absence (MI) or presence of acetylcholine (MI + ACh) at basic cycle length (500 milliseconds) and with shorter (500/150 milliseconds) coupling intervals. A: Normal anisotropic conduction from the pacing site in the baseline at BCL = 500 milliseconds and with shorter (500/150 milliseconds) coupling intervals. B: MI prolonged activation time in the IBZ, especially at shorter coupling intervals. C: ACh prevented ischemia-induced prolongation of the activation time in the IBZ even with shorter coupling intervals. D–F: Relationship between pacing coupling interval (S1–S2) and averaged CV in the NIZ or IBZ in each group. CV in the IBZ was significantly slower than the baseline, whereas that in MI+ ACh was not decreased. CV in the shorter coupling interval was significantly slower than that of the BCL in the baseline and after MI, whereas CV did not slow in MI+ ACh even in the shorter coupling interval. The area with the diagonal line indicates the ischemic zone (IZ). *P < 0.05 vs. baseline, †P < 0.05 vs. BCL = 500 milliseconds. For a high quality, full color version of this figure, please see Journal of Cardiovascular Electrophysiology's website: www.wileyonlinelibrary.com/journal/jce*

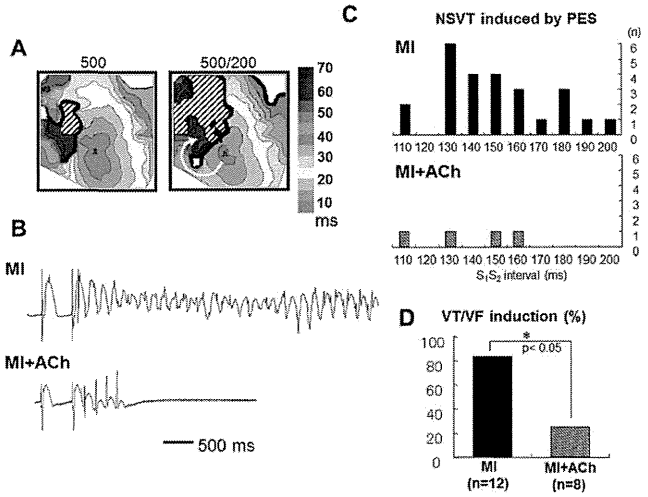

Figure 3. *VT/VF susceptibility by PES after MI in absence or presence of ACh. A: Optical isochronal activation map after myocardial ischemia (MI) by LAD coronary artery ligation at basic cycle length (500 milliseconds) and with a shorter coupling interval (500/200 milliseconds). MI induced a severe conduction delay and the shorter coupling interval induced uni-directional conduction block in the ischemic border zone. B–D: Representative electrocardiograms of VT/VF after MI or MI + ACh induced by programmed electrical stimulation (PES) (B), and frequency of nonsustained VT (NSVT) (C) and sustained VT/VF (D) induced by PES after MI or MI+ACh. For a high quality, full color version of this figure, please see Journal of Cardiovascular Electrophysiology's website: www.wileyonlinelibrary.com/journal/jce*

TABLE 1
Effect of ACh on Repolarization Parameters After MI

	APD_{75} (Milliseconds) (BCL = 500 Milliseconds)				
	Max.	Min.	Mean	Mean (IBZ)	ERP (Milliseconds)
Baseline	178 ± 23	129 ± 9	150 ± 18	–	144 ± 10
MI	161 ± 21	66 ± 15*	115 ± 19*	115 ± 13	130 ± 23
MI + ACh	176 ± 23	63 ± 7*	110 ± 6*	99 ± 6	130 ± 18

APD_{75} = action potential duration at 75% repolarization; IBZ = ischemic border zone; ERP = effective refractory period; MI = myocardial ischemia; ACh = acetylcholine.
*P < 0.05 vs. baseline.

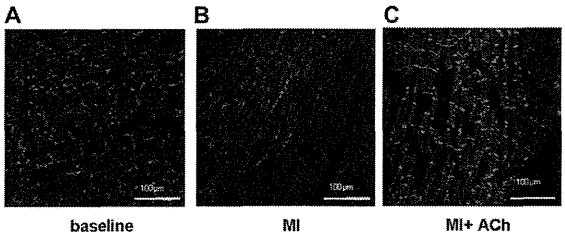

Figure 4. *Effect of ACh on Cx43 localization. Representative confocal images of rabbit anterior left ventricles in the baseline (A), after myocardial ischemia (MI) in the absence (B) and presence of acetylcholine (MI + ACh) (C). Positive immunoreactive signals were concentrated in discrete spots at sites of intercellular apposition (red). For a high quality, full color version of this figure, please see Journal of Cardiovascular Electrophysiology's website: www.wileyonlinelibrary.com/journal/jce*

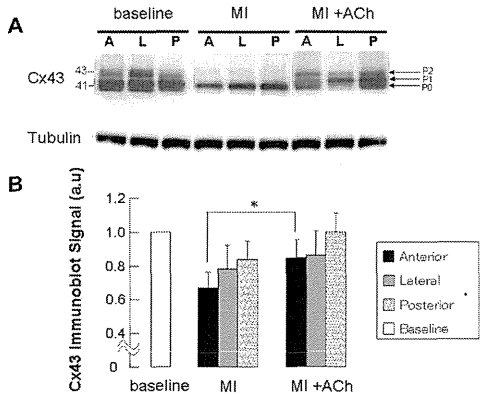

Figure 5. *A: Representative immunoblots of homogenate of rabbit anterior (A), lateral (L), and posterior (P) left ventricles in the baseline, 30 minutes after myocardial ischemia (MI), and after MI with ACh (MI + ACh). Samples show multiple Cx43 protein bands (P0, P1 and P2) depending on the phosphorylation level, thus the lower molecular weight-band (P0) represents nonphosphorylated and higher-band (P1 and P2) represent phosphorylated isoform of Cx43. MI decreased phosphorylated Cx43, especially in the anterior region. ACh treatment prevented MI-induced loss of phosphorylated Cx43. B: Quantitative densitometric analysis of the phosphorylated isoform of Cx43 after MI and MI + ACh. a.u. = arbitrary units. For a high quality, full color version of this figure, please see Journal of Cardiovascular Electrophysiology's website: www.wileyonlinelibrary.com/journal/jce*

Effect of Acetylcholine on Cx43 Localization and Expression

To investigate the distribution of Cx43 during acute MI with or without ACh, we performed confocal image analysis of LV tissues stained with anti-Cx43 antibody. As shown in Figure 4A, the localization of immunoreactive signals in the baseline was restricted to intercellular junctions, consistent with the gap junctions and intercalated disk. In contrast, the Cx43 signal was reduced dramatically in the anterior region after MI (Fig. 4B); however, the Cx43 signal in the anterior region after MI with ACh was almost similar to the level of the control (Fig. 4C). These observations indicate that the loss of phosphorylated Cx43 during acute MI was prevented by ACh treatment.

Figure 5A depicts a representative immunoblot prepared with anti-Cx43 antibody. Acute MI significantly downregulated the phosphorylated isoform of Cx43 (bands with 43 kDa), especially in the anterior region, compared with that of the baseline. However, ACh prevented the MI-induced downregulation of the phosphorylated isoform of Cx43 in the anterior region. Figure 5B depicts a normalized quantitative densitometric analysis of the phosphorylated isoform of Cx43. MI reduced Cx43 in the anterior, lateral, and posterior regions at 66 ± 21%, 78 ± 31%, and 83 ± 26% of the baseline, respectively. However, ACh maintained Cx43 in each region at 85 ± 24% ($P < 0.05$ vs. MI anterior), 86 ± 32%, and 99 ± 25% of the baseline, respectively.

Discussion

The present findings support the hypothesis that (1) ischemia-induced conduction slowing and arrhythmogenesis are a partial consequence of the Cx43 remodeling of IBZ, (2) ACh, a vagal efferent neurotransmitter, can attenuate acute MI-induced slower CV and arrhythmogenic substrate by maintaining a principal cardiac gap junction protein, Cx43, in the IBZ. Furthermore, it is of note that these electrophysiological results are obtained in the physiological condition with a freely beating heart without elimination of the contractility with a motion blocker. Although there are many other factors which may contribute to antiarrhythmic effects of ACh during ischemia, this study suggests that one of the possible mechanisms is preservation of Gap junction protein, Cx43 in the IBZ.

Mechanisms of ACh in Preventing Ischemia-Induced Arrhythmia

Heart Rate

Vagal nerve stimulation has already been reported to prevent VF in dogs with acute or chronic MI[22] and in rats with heart failure.[24] One of the reasons for the vagal nerve stimulation-induced antiarrhythmic effect is considered to be its bradycardiac effect.[28] Vagal nerve stimulation

or ACh shortens APD by I_{KACh} in atrium but not ventricle, thus may increase risk of atrial fibrillation,[29] In contrast for ventricle, these are cardioprotective and antiarrhythmic during ischemia or heart failure.[16] Our previous study demonstrated that vagal stimulation and ACh are cardioprotective independent from the heart rate slowing during hypoxia or ischemia,[17] which is consistent with the findings of this study that the suppression of PES-induced arrhythmias after acute MI is associated with the maintaining of CV by ACh. As such, the antiarrhythmic effect of ACh seems to be independent from its bradycardiac effect.

Gap Junction and Cx43 Preservation

Gap junction channels, which are composed of highly homologous proteins known as connexins in vertebrate species, have been implicated in the electrical coupling of excitable tissues, such as cardiac muscles.[6] The protein content of ventricular Cx43 is remarkably reduced in ischemia[6,10] and heart failure.[30] In experimental preparation, cell uncoupling via reduced gap junction typically begins ~15 minutes after the onset of ischemia and may continue for 30 or 40 minutes, when cell injury becomes irreversible.[31] Cx43 is a protein with a half-life of only 1 to 3 h in the adult heart. ACh may suppress the degradation pathway of Cx43 during acute MI.[17] In this study, we demonstrated the regional differences in the electrophysiological characteristics of CV and APD at the baseline and 30 minutes after coronary artery ligation with or without ACh, which can produce the electrophysiological heterogeneity between the IZ and the NIZ within the ventricular wall. Most notably, we investigated the arrhythmogenic substrate in the IBZ during acute regional MI. These results are consistent with those of the previous report that demonstrated that stimulation of the cardiac M3-muscarinic ACh receptor prevented ischemia-induced arrhythmia by preserving phosphorylate-Cx43.[32]

Slow conduction caused by abnormal gap junction coupling of ischemia-related cultured myocytes[8] or myocardium[10] is thought to be a component of the arrhythmogenic substrate. Cx43-deficient mice exhibited earlier and higher incidence of VT/VF than wild-type mice during acute regional MI,[33,34] and moderate to severe reductions in Cx43 abundance in Cx43 knock-out mice were associated with a slowing of impulse propagation and an increase in the susceptibility to inducible VT/VF.[35] Increasing the spatial CV dispersion by impairing the regional gap junctional conductance increased the defibrillation threshold.[36] Consistent with previous results, the heterogeneous reduction of gap junctions in this study was associated with slower CV and higher incidence of uni-directional conduction block in the IBZ, leading to VT/VF. ACh markedly improved the loss of gap junction in the IBZ, thus reducing VT/VF induction. In addition, ACh treatment might reduce anisotropy of ventricular conduction since CV was preserved not only in the long axis but also in the short axis. This study did not analyze ACh-induced cellular re-distribution of gap junction; however, it might change the anisotropy of conduction.

Although this study did not evaluate the role of regional MI in the maintenance of VF, the previous results suggested that the heterogeneity of CV and APD in regional MI lead to the coexistence of 2 types of VF,[9] and the IBZ was in regions with a steep APD restitution slope and unstable calcium dynamics, leading to the increase in the wave break of spiral re-entry[37] and the maintained VF.[11]

Other Potential Mechanisms

In this study we focused on preservation of gap junction protein, Cx43 in IBZ by ACh treatment. However, there are many other factors which could explain or at least contribute to the suppression of VT/VF by ACh. One potential mechanism of protection against ischemia-reperfusion injury by ACh is mediated by nitric oxide (NO) synthesis.[38,39] NO mediated vasodilatory effects which would expected to alter coronary perfusion into ischemic zone. Thus, improved conduction velocity could be simply due to less severe ischemic damage by ACh. NO and O_2 radicals activate the PKC-ε isoform by which ACh protects myocytes against ischemic injury.[40] PKC-ε directly phosphorylates Cx43, and PKC-ε plays a critical role in preconditioning to preserve the Cx43 signal in gap junctions, thus maintaining electrical coupling during ischemia.[41] Moreover, ACh reduces contractility that would also reduce the metabolic demand on the heart at a time when ATP supply is low. A recent paper suggested that vagus nerve stimulation during ischemia exerts cardioprotection by reduction of cardiac mitochondrial reactive oxygen species production.[42] Thus, this energetic benefit would be expected to be cardioprotective as well.

Influence of Motion Blocker

There are several commonly used motion-suppressing agents including 2,3-butanedione monoxime (BDM), Cytochalasin D and Blebbistatin for optical mapping. BDM is known to inhibit many ionic currents at concentrations required to reduce motion artifacts. Furthermore, BDM provides a protective effect during reperfusion after ischemia.[43] On the other hand, cytochalasin D is a well-known inhibitor of actin polymerization and a disruptor of actin cytoskeleton, which affects Ca^{2+} and K_{ATP} channels as well as Cx trafficking.[44-46] Moreover, cytochalasin D and BDM may affect the dephosphorylation of Cx43.[44,47,48] These findings suggest that BDM and cytochalasin D may affect MI-induced changes of repolarization and depolarization. In this study, we recorded the optical APs with a freely beating rabbit heart without using motion blockers. We reduced motion artifacts through our novel tracking and ratiometric methods[25] and were thus able to obtain the ischemia-induced electrophysiological changes in physiological conditions.

Study Limitations

There were several limitations in this study. First, ligation of the left anterior descending coronary artery induces regional ischemia; however, the ischemic region was heterogeneous depending on the anatomy of the coronary artery, and we evaluated the LV epicardial surface only, not the transmural differences, although TTC staining was performed in some isolated rabbit hearts to directly confirm the infarct areas (Supporting Fig. S2) compared with electrophysiological ischemic zone. Thus, the actual IBZ and its CV is difficult to determine. Moreover, this study evaluated VT/VF inducibility and carried out an electrophysiological characterization of 30 minutes regional ischemia, but not the arrhythmogenic substrate in the IBZ of healed myocardial infarction.

Second, we started a perfusion of ACh 5 minutes before ligation; thus pretreatment of ACh may reduce the ischemic area resulting in decreasing the area of slower CV and we did not evaluate the effect of ACh on the ischemic size. Furthermore, ACh can affect the cardiac sodium channel

function and maintain the CV in IBZ. Third, we performed single extra stimulus (S1–S2) of 10 milliseconds decrement protocol because this optical mapping system needed much time and memory space to store the data, which might fail to detect the precise refractory period, trigger and vulnerability of reentrant arrhythmias.

References

1. Zipes DP, Wellens HJ: Sudden cardiac death. Circulation 1998;98: 2334-2351.
2. Echt DS, Liebson PR, Mitchell LB, Peters RW, Obias-Manno D, Barker AH, Arensberg D, Baker A, Friedman L, Greene HL, Huther ML, Richardson DW and the CAST Investigators: Mortality and morbidity in patients receiving encainide, flecainide, or placebo. The cardiac arrhythmia suppression trial. N Engl J Med 1991;324:781-788.
3. Yan GX, Kleber AG: Changes in extracellular and intracellular pH in ischemic rabbit papillary muscle. Circ Res 1992;71:460-470.
4. Dekker LR, Fiolet JW, VanBavel E, Coronel R, Opthof T, Spaan JA, Janse MJ: Intracellular Ca2+, intercellular electrical coupling, and mechanical activity in ischemic rabbit papillary muscle. Effects of preconditioning and metabolic blockade. Circ Res 1996;79:237-246.
5. Remme WJ: The sympathetic nervous system and ischaemic heart disease. Eur Heart J 1998;19(Suppl F):F62-F71.
6. Saffitz JE, Lerner DL, Yamada KA: Gap junction distribution and regulation in the heart. In: Zipes DP, Jalife J, eds. *Cardiac Electrophysiology: From Cell to Bedside*, 4th ed. Philadelphia: WB Saunders; 2004, pp. 181-191.
7. Cabo C, Yao J, Boyden PA, Chen S, Hussain W, Duffy HS, Ciaccio EJ, Peters NS, Wit AL: Heterogeneous gap junction remodeling in reentrant circuits in the epicardial border zone of the healing canine infarct. Cardiovasc Res 2006;72:241-249.
8. Zeevi-Levin N, Barac YD, Reisner Y, Reiter I, Yaniv G, Meiry G, Abassi Z, Kostin S, Schaper J, Rosen MR, Resnick N, Binah O: Gap junctional remodeling by hypoxia in cultured neonatal rat ventricular myocytes. Cardiovasc Res 2005;66:64-73.
9. Liu YB, Pak HN, Lamp ST, Okuyama Y, Hayashi H, Wu TJ, Weiss JN, Chen PS, Lin SF: Coexistence of two types of ventricular fibrillation during acute regional ischemia in rabbit ventricle. J Cardiovasc Electrophysiol 2004;15:1433-1440.
10. De Groot JR, Coronel R: Acute ischemia-induced gap junctional uncoupling and arrhythmogenesis. Cardiovasc Res 2004;62:323-334.
11. Zaitsev AV, Guha PK, Sarmast F, Kolli A, Berenfeld O, Pertsov AM, de Groot JR, Coronel R, Jalife J: Wavebreak formation during ventricular fibrillation in the isolated, regionally ischemic pig heart. Circ Res 2003;92:546-553.
12. Yao JA, Hussain W, Patel P, Peters NS, Boyden PA, Wit AL: Remodeling of gap junctional channel function in epicardial border zone of healing canine infarcts. Circ Res 2003;92:437-443.
13. Ohara T, Ohara K, Cao JM, Lee MH, Fishbein MC, Mandel WJ, Chen PS, Karagueuzian HS: Increased wave break during ventricular fibrillation in the epicardial border zone of hearts with healed myocardial infarction. Circulation 2001;103:1465-1472.
14. Peters NS, Wit AL: Gap junction remodeling in infarction: Does it play a role in arrhythmogenesis? J Cardiovasc Electrophysiol 2000;11:488-490.
15. Zipes DP, Rubart M: Neural modulation of cardiac arrhythmias and sudden cardiac death. Heart Rhythm 2006;3:108-113.
16. Li M, Zheng C, Sato T, Kawada T, Sugimachi M, Sunagawa K: Vagal nerve stimulation markedly improves long-term survival after chronic heart failure in rats. Circulation 2004;109:120-124.
17. Ando M, Katare RG, Kakinuma Y, Zhang D, Yamasaki F, Muramoto K, Sato T: Efferent vagal nerve stimulation protects heart against ischemia-induced arrhythmias by preserving connexin43 protein. Circulation 2005;112:164-170.
18. Kakinuma Y, Ando M, Kuwabara M, Katare RG, Okudela K, Kobayashi M, Sato T: Acetylcholine from vagal stimulation protects cardiomyocytes against ischemia and hypoxia involving additive non-hypoxic induction of hif-1alpha. FEBS Lett 2005;579:2111-2118.
19. Zhang Y, Kakinuma Y, Ando M, Katare RG, Yamasaki F, Sugiura T, Sato T: Acetylcholine inhibits the hypoxia-induced reduction of connexin43 protein in rat cardiomyocytes. J Pharmacol Sci 2006;101:214-222.
20. Takahashi N, Ito M, Ishida S, Fujino T, Saikawa T, Arita M: Effects of vagal stimulation on cesium-induced early afterdepolarizations and ventricular arrhythmias in rabbits. Circulation 1992;86:1987-1992.
21. Myers RW, Pearlman AS, Hyman RM, Goldstein RA, Kent KM, Goldstein RE, Epstein SE: Beneficial effects of vagal stimulation and bradycardia during experimental acute myocardial ischemia. Circulation 1974;49:943-947.
22. Vanoli E, De Ferrari GM, Stramba-Badiale M, Hull SS Jr, Foreman RD, Schwartz PJ: Vagal stimulation and prevention of sudden death in conscious dogs with a healed myocardial infarction. Circ Res 1991;68:1471-1481.
23. Rosenshtraukh L, Danilo P Jr, Anyukhovsky EP, Steinberg SF, Rybin V, Brittain-Valenti K, Molina-Viamonte V, Rosen MR: Mechanisms for vagal modulation of ventricular repolarization and of coronary occlusion-induced lethal arrhythmias in cats. Circ Res 1994;75:722-732.
24. Zheng C, Li M, Inagaki M, Kawada T, Sunagawa K, Sugimachi M: Vagal stimulation markedly suppresses arrhythmias in conscious rats with chronic heart failure after myocardial infarction. Conf Proc IEEE Eng Med Biol Soc 2005;7:7072-7075.
25. Inagaki M, Hidaka I, Aiba T, Tatewaki T, Sunagawa K, Sugimachi M: High resolution optical mapping of cardiac action potentials in freely beating rabbit hearts. Conf Proc IEEE Eng Med Biol Soc 2004;5:3578-3580.
26. Aiba T, Shimizu W, Hidaka I, Uemura K, Noda T, Zheng C, Kamiya A, Inagaki M, Sugimachi M, Sunagawa K: Cellular basis for trigger and maintenance of ventricular fibrillation in the brugada syndrome model: High-resolution optical mapping study. J Am Coll Cardiol 2006;47:2074-2085.
27. Seo K, Inagaki M, Nishimura S, Hidaka I, Sugimachi M, Hisada T, Sugiura S: Structural heterogeneity in the ventricular wall plays a significant role in the initiation of stretch-induced arrhythmias in perfused rabbit right ventricular tissues and whole heart preparations. Circ Res.2010;106:176-184.
28. Zuanetti G, De Ferrari GM, Priori SG, Schwartz PJ: Protective effect of vagal stimulation on reperfusion arrhythmias in cats. Circ Res 1987;61:429-435.
29. Rosenshtraukh LV, Zaitsev AV, Fast VG, Pertsov AM, Krinsky VI: Vagally induced block and delayed conduction as a mechanism for circus movement tachycardia in frog atria. Circ Res 1989;64:213-226.
30. Akar FG, Nass RD, Hahn S, Cingolani E, Shah M, Hesketh GG, Disilvestre D, Tunin RS, Kass DA, Tomaselli GF: Dynamic changes in conduction velocity and gap junction properties during development of pacing induced heart failure. Am J Physiol Heart Circ Physiol 2007;293:H1223-H1230.
31. Beardslee MA, Lerner DL, Tadros PN, Laing JG, Beyer EC, Yamada KA, Kleber AG, Schuessler RB, Saffitz JE: Dephosphorylation and intracellular redistribution of ventricular connexin43 during electrical uncoupling induced by ischemia. Circ Res 2000;87:656-662.
32. Zhao J, Su Y, Zhang Y, Pan Z, Yang L, Chen X, Liu Y, Lu Y, Du Z, Yang B: Activation of cardiac muscarinic M3 receptors induces delayed cardioprotection by preserving phosphorylated connexin43 and up-regulating cyclooxygenase-2 expression. Br J Pharmacol 2010;159:1217-1225.
33. Lerner DL, Yamada KA, Schuessler RB, Saffitz JE: Accelerated onset and increased incidence of ventricular arrhythmias induced by ischemia in Cx43-deficient mice. Circulation 2000;101:547-552.
34. Betsuyaku T, Kanno S, Lerner DL, Schuessler RB, Saffitz JE, Yamada KA: Spontaneous and inducible ventricular arrhythmias after myocardial infarction in mice. Cardiovasc Pathol 2004;13:156-164.
35. Danik SB, Liu F, Zhang J, Suk HJ, Morley GE, Fishman GI, Gutstein DE: Modulation of cardiac gap junction expression and arrhythmic susceptibility. Circ Res 2004;95:1035-1041.
36. Sims JJ, Schoff KL, Loeb JM, Wiegert NA: Regional gap junction inhibition increases defibrillation thresholds. Am J Physiol Heart Circ Physiol 2003;285:H10-16.
37. Chou CC, Zhou S, Hayashi H, Nihei M, Liu YB, Wen MS, Yeh SJ, Fishbein MC, Weiss JN, Lin SF, Wu D, Chen PS: Remodelling of action potential and intracellular calcium cycling dynamics during subacute myocardial infarction promotes ventricular arrhythmias in langendorff-perfused rabbit hearts. J Physiol 2007;580:895-906.
38. Chowdhary S, Townend JN: Role of nitric oxide in the regulation of cardiovascular autonomic control. Clin Sci (Lond) 1999;97:5-17.
39. Brack KE, Patel VH, Coote JH, Ng GA: Nitric oxide mediates the vagal protective effect on ventricular fibrillation via effects on action potential duration restitution in the rabbit heart. J Physiol 2007;583:695-704.

40. Liu H, McPherson BC, Zhu X, Da Costa ML, Jeevanandam V, Yao Z: Role of nitric oxide and protein kinase c in ach-induced cardioprotection. Am J Physiol Heart Circ Physiol 2001;281:H191-197.
41. Hund TJ, Lerner DL, Yamada KA, Schuessler RB, Saffitz JE: Protein kinase cepsilon mediates salutary effects on electrical coupling induced by ischemic preconditioning. Heart Rhythm 2007;4:1183-1193.
42. Shinlapawittayatorn K, Chinda K, Palee S, Surinkaew S, Kumfu S, Kumphune S, Chattipakorn S, KenKnight BH, Chattipakorn N: Vagus nerve stimulation initiated late during ischemia, but not reperfusion, exerts cardioprotection via amelioration of cardiac mitochondrial dysfunction. Heart Rhythm 2014;11:2278-2287.
43. Boban M, Stowe DF, Kampine JP, Goldberg AH, Bosnjak ZJ: Effects of 2,3-butanedione monoxime in isolated hearts: Protection during reperfusion after global ischemia. J Thorac Cardiovasc Surg 1993;105:532-540.
44. Rueckschloss U, Isenberg G: Cytochalasin d reduces Ca2+ currents via cofilin-activated depolymerization of f-actin in guinea-pig cardiomyocytes. J Physiol 2001;537:363-370.
45. Nygren A, Baczko I, Giles WR: Measurements of electrophysiological effects of components of acute ischemia in Langendorff-perfused rat hearts using voltage-sensitive dye mapping. J Cardiovasc Electrophysiol 2006;17(Suppl 1):S113-S123.
46. Gilleron J, Nebout M, Scarabelli L, Senegas-Balas F, Palmero S, Segretain D, Pointis G: A potential novel mechanism involving connexin 43 gap junction for control of sertoli cell proliferation by thyroid hormones. J Cell Physiol 2006;209:153-161.
47. Casella JF, Flanagan MD, Lin S: Cytochalasin d inhibits actin polymerization and induces depolymerization of actin filaments formed during platelet shape change. Nature 1981;293:302-305.
48. Verrecchia F, Herve JC: Reversible blockade of gap junctional communication by 2,3-butanedione monoxime in rat cardiac myocytes. Am J Physiol 1997;272:C875-C885.

Supporting Information

Additional supporting information may be found in the online version of this article at the publisher's website:

Figure S1. Reduction of motion artifact by tracking methods. A: Several small beads (0.5 mm ϕ) were placed on the epicardial surface as landmarks. B: These landmarks were manually detected in the first frame (left, red boxes) and then automatically tracked by computer software in each frame (right, blue boxes) during optical recording. C: The displacement vector of the observatory point at frame t, (D(t)) was predicted by the weighted sum of the displacement vectors of the markers.

Figure S2. Histological confirmation for the ischemic area. A: Optical mapping in isolated rabbit ventricular heart during myocardial ischemia (MI) by left anterior descending (LAD) coronary artery ligation. B: Optical brightness of the rabbit ventricle during MI by LAD ligation. C: Infarct area of LV anterior was shown as a non-staining area by Triphenyltetrazolium chloride (TTC).

Journal of Arrhythmia 32 (2016) 70–73

Contents lists available at ScienceDirect

Journal of Arrhythmia

journal homepage: www.elsevier.com/locate/joa

Case Report

An overlap of Brugada syndrome and arrhythmogenic right ventricular cardiomyopathy/dysplasia

Shohei Kataoka, MD*, Naoki Serizawa, MD, Kazutaka Kitamura, MD, Atsushi Suzuki, MD, Tsuyoshi Suzuki, MD, Tsuyoshi Shiga, MD, Morio Shoda, MD, Nobuhisa Hagiwara, MD

Department of Cardiology, Tokyo Women's Medical University, 8-1 Kawadacho, Shinjuku-ku, Tokyo 162-8666, Japan

ARTICLE INFO

Article history:
Received 15 July 2015
Received in revised form
25 October 2015
Accepted 29 October 2015
Available online 30 November 2015

Keywords:
Brugada syndrome
Arrhythmogenic right ventricular cardiomyopathy/dysplasia
An overlap disease

ABSTRACT

Overlapping characteristics of Brugada syndrome (BrS) and arrhythmogenic right ventricular cardiomyopathy/dysplasia (ARVC/D) have been reported in recent studies, but little is known about the overlapping disease state of BrS and ARVC/D. A 36-year-old man, hospitalized at our institution for syncope, presented with this overlapping disease state. The electrocardiogram showed spontaneous coved-type ST-segment elevation, and ventricular fibrillation was induced by right ventricular outflow tract stimulation in an electrophysiological study. BrS was subsequently diagnosed; additionally, the presence of epsilon-like waves and right ventricular structural abnormalities met with the 2010 revised task force criteria for ARVC/D. After careful investigation for both BrS and ARVC/D, an implantable cardioverter defibrillator was inserted in the patient. This case revealed 2 important clinical findings: (1) BrS and ARVC/D clinical features can coexist in a single patient, and EPS might be useful for determining the phenotype of overlapping disease (e.g., BrS-like or ARVC/D-like). (2) An overlapping disease state of BrS and ARVC/D can change phenotypically during its clinical course. Therefore, careful examination and attentive follow-up are required for patients with BrS or ARVC/D.

1. Introduction

Brugada syndrome (BrS) is characterized by right precordial ST-segment elevation followed by a negative T wave and sudden cardiac death from ventricular fibrillation in patients with structurally normal hearts [1]. Recent studies have revealed structural or electrocardiographic abnormalities, such as right ventricular dilatation or epsilon-like waves, in some patients with BrS [2,3]. These abnormalities are commonly considered characteristics of arrhythmogenic right ventricular cardiomyopathy/dysplasia (ARVC/D). It is generally known that there are clinical similarities between BrS and ARVC/D [4]; however, little is known about the clinical features of patients with an overlapping disease state of BrS and ARVC/D, and accordingly, treatment of such patients remains poorly understood. In order to understand this condition better, we report here, a case of overlapping disease state of BrS and ARVC/D.

2. Case report

A 36-year-old man presented to our institution with syncope, and was subsequently, hospitalized. He had no family history of sudden cardiac death. The electrocardiogram (ECG) showed spontaneous coved-type ST-segment elevation (Brugada type 1 ECG); we initially suspected BrS. In an electrophysiological study (EPS) conducted prior to pilsicainide infusion, neither ventricular tachycardia (VT) nor ventricular fibrillation (VF) was induced by a single or double stimulus to the right ventricular apex or right ventricular outflow tract. A single stimulus to the right ventricular outflow tract during pilsicainide infusion induced ventricular fibrillation, which was thereafter, inhibited during isoproterenol infusion. Therefore, the patient was diagnosed with BrS, although the clinical presentation differed from typical BrS to some extent. First, the chest radiograph and cardiovascular magnetic resonance imaging (CMR) showed mild right ventricular (RV) dilatation (Fig.1A, B). Second, RV angiography demonstrated RV dilatation and akinesis in the inferior wall (Fig.1C, D), although coronary angiography did not show critical stenosis, and the provocation test failed to induce coronary spasm. Finally, epsilon-like waves were seen in spontaneous type 1 ECG (Fig.2). As a result, the patient not only met the diagnostic criteria for BrS but also met the

* Corresponding author. Tel.: +81 3 3353 8111; fax: +81 3 3353 6793.
E-mail address: shoheikataoka0818@gmail.com (S. Kataoka).

http://dx.doi.org/10.1016/j.joa.2015.10.007

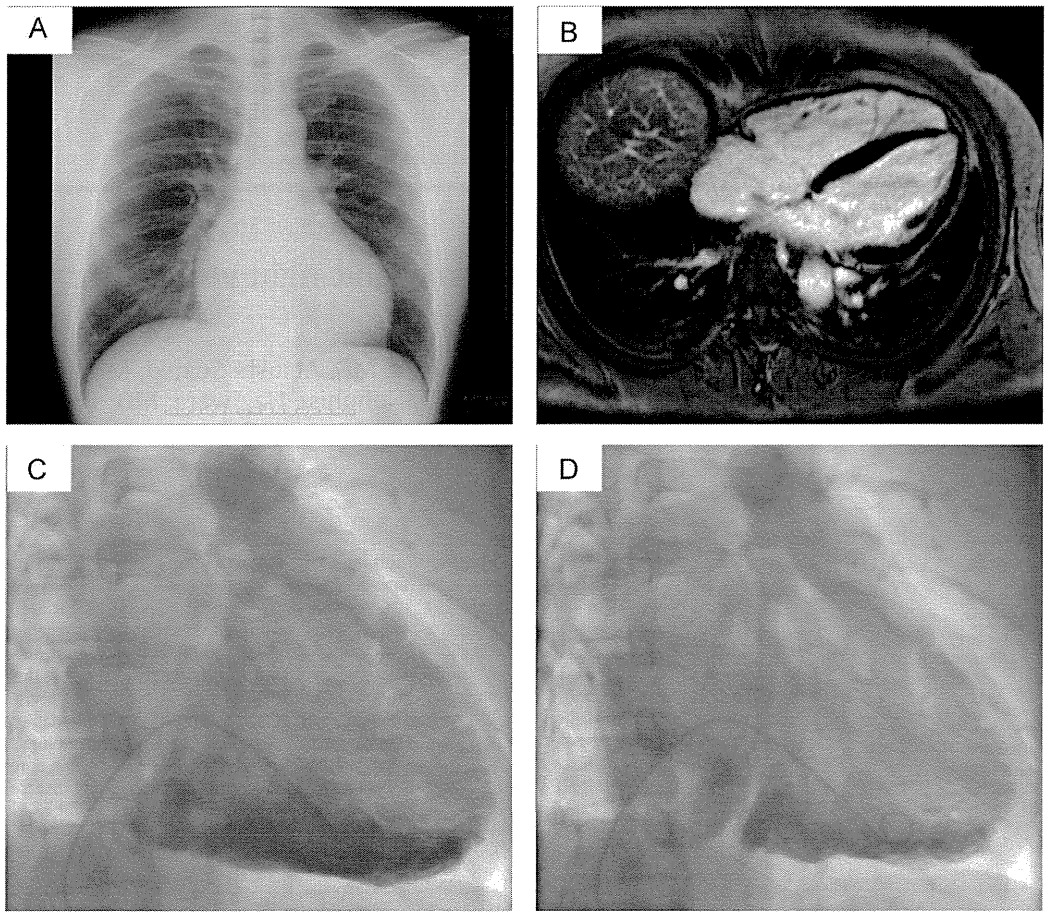

Fig. 1. (A)Chest radiograph reveals mild right ventricle dilatation. (B) Cardiovascular magnetic resonance imaging shows mild right ventricle dilatation and no late gadolinium enhancement. (C) Right ventricular angiography demonstrates right ventricular dilatation and akinesis in the inferior wall. (D) Computed tomography does not reveal fatty change in the right ventricular myocardium.

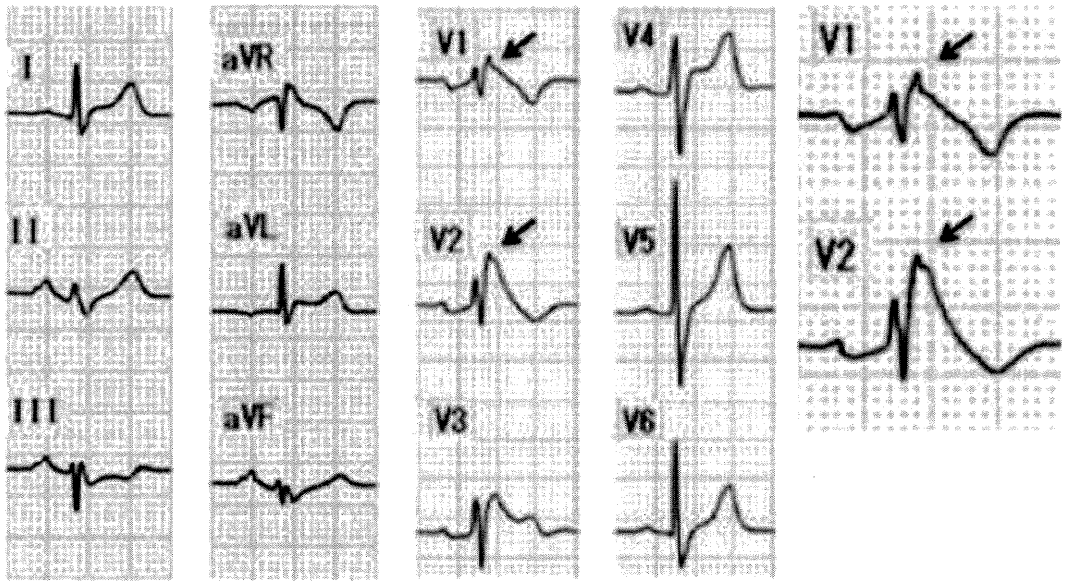

Fig. 2. The patient's electrocardiogram shows spontaneous coved-type ST-segment elevation and epsilon-like waves in type 1 ECG.

Table 1
Clinical characteristics of the present case.

Age at presentation		36 years old
Sex		Male
QTc		416 ms
Head-up tilt test		Negative
Atrial arrhythmias		None
AV conduction		Normal
CAG		No significant stenosis
LVEF		47%
RVEF		43%
LVEDV(I) / ESV(I)		136(76) / 68(39) ml (ml/m^2)
RVEDV(I) / ESV(I)		233(134) / 134(77) ml (ml/m^2)
Spasm provocation test		Negative
CMR		No Late gadolinium enhancement
Characteristics of ARVC / D	Symptoms	Syncope
	Family history of ARVC/D	None
	RV angiography	Regional RV akinesis
	ECG depolarization	Epsilon wave
	Late potentials	f-QRS=174 ms, LAS40=79 ms, RMS40=7.7 μV
	ECG changes	Fixed
	Imaging	RV dilatation
	Gene mutation of ARVC/D	None
Characteristics of BrS	Symptoms	Syncope
	Family history of SCD	None
	Family history of BrS	None
	ECG repolarization	Spontaneous coved-type ST segment elevation
	Ventricular arrhythmias	VF/Polymorphic VT (induced in the EPS)
	Beta-stimulation	Inhibited (in the EPS)
	Pathology	Not specific
	Gene mutation of BrS	None

ARVC/D=Arrhythmogenic right ventricular cardiomyopathy/dysplasia , AV conduction=atrioventricular conduction, BrS=Brugada syndrome, CAG=coronary angiography, CMR=cardiovascular magnetic resonance, EPS=electrophysiological study, f-QRS=filtered QRS, LAS40=duration of terminal QRS < 40 μV, LVEF=left ventricular ejection fraction, LVEDV (I)=left ventricular end-diastolic volume (index), LVESV(I)=left ventricular end-systolic volume(index), QTc=corrected QT interval, RMS40=root-mean-square voltage of terminal 40 ms, RV=right ventricle, RVEF=right ventricular ejection fraction, RVEDV(I)=right ventricular end-diastolic volume(index), RVESV(I)=right ventricular end-systolic volume(index), SCD=sudden cardiac death, VF=ventricular fibrillation, VT=ventricular tachycardia

2 major parameters of 2010 revised task force criteria for ARVC/D (regional RV akinesis by RV angiography and the presence of an epsilon wave in the right precordial leads). The patient was discharged from the hospital after insertion of an implantable cardioverter defibrillator (ICD).

3. Discussion

In this case study, we determined 2 important clinical issues. First, the phenotype of an overlapping disease state for BrS and ARVC/D may vary between individuals, and therefore, EPS may be useful for determining the phenotype of an overlapping disease (e.g., BrS-like or ARVC/D-like). Second, careful examination is needed to confirm diagnosis in the cases suspected of overlapping BrS and ARVC/D, and to determine better treatment course for these patients.

Although presentation of the overlapping disease state may vary among patients, past investigations have demonstrated some common features of the overlap. First, sodium channel blockers can induce BrS ECG in a subgroup of patients with ARVC/D [5], and epsilon-like waves are seen in some patients with type 1 ECG. Epsilon-like waves are more common in drug-induced type 1 ECGs than in spontaneous type 1 ECGs [3]. Rather than using the term "epsilon wave," we use the term "epsilon-like wave" because distinguishing the epsilon wave from the fragmented QRS wave was difficult. The epsilon wave is located between the end of the QRS complex and beginning of the T-wave. In contrast, a fragmented QRS (f-QRS) is defined as the presence of additional spikes within the QRS complex. In patients with BrS, defining the end of QRS complex is difficult, and it is still controversial where the J wave represents depolarization component or repolarization component. Therefore, occurrence of additional spikes at the end of QRS complex or immediately after the QRS complex in BrS is not certain. The term "epsilon-like wave" has been used to avoid such discrepancies in ECG interpretation. [3] Some previous studies revealed that epsilon potentials and QRS fragmentation have similarly high diagnostic values, and epsilon-like potentials in different leads at the beginning, top, or end of the QRS complex are typical ECG findings in patients with ARVC/D. [6,7]. Second, imaging studies have revealed RV wall motion abnormalities or RV dilatation, which are characteristic of ARVC/D, in some patients with BrS [2,8]. Third, the fibro-fatty replacements required to diagnose ARVC/D have been detected during endocardial biopsies of patients with type 1 ECG [9]. Finally, specific gene mutations involving ARVC/D have been identified in some patients with BrS [10]. These overlapping features are considered a result either of genetic interactions or of the combined influence of BrS' electrophysiological abnormalities and ARVC/D's structural abnormalities. Accordingly, ARVC/D patients can satisfy the diagnostic criteria of BrS, and BrS patients can satisfy the diagnostic criteria of ARVC/D.

A disease state combining both conditions has a different clinical course than uncomplicated BrS. A subgroup of BrS patients may demonstrate the features of ARVC/D long after the initial BrS diagnosis. Structural heart diseases and histological findings consistent with ARVC/D have been revealed after autopsy of patients who were diagnosed with BrS and who died suddenly [11]. Thus, careful observation of the changing clinical course is vital and may indicate the transformation from BrS to ARVC/D.

Detailed evaluation in the cases of suspected overlap of BrS and ARVC/D is also needed to determine a better treatment course for these patients. In this case, we used a range of methods, from physical examination to genetic testing (BrS- and ARVC/D-specific), to confirm dual diagnosis and to determine a better course

Table 2
Analyzed gene mutations.

Gene	Phenotype
RYR2	CPVT1/ARVC2
SCN5A	LQTS/BrS1
CACNA1C	LQT8/BrS3
CACNB2	BrS4
CACNA2D1	BrS9
SCN1B	BrS5
SCN3B	BrS7
GPD1L	BrS2
KCND3	BrS10
KCNJ8	ERS1/BrS8
KCNE3	BrS6
KCNE4	
KCNE5	BrS/IVF
SCN10A	BrS
MOG1 (RANGRF)	BrS11
DSP	ARVC8
PKP2	ARVC9
DSG2	ARVC10
DSC2	ARVC11
JUP	ARVC12

of treatment (Tables 1, 2). Since this patient experienced an episode of syncope, demonstrated epsilon-like waves in spontaneous type 1 ECG, and showed RV dilatation and RV wall motion abnormalities, a diagnosis of overlap disease of BrS and ARVC/D for the patient can be asserted with certainty.

Although treating patients with BrS features in the case of structural heart disease remains challenging, this patient received an ICD because of spontaneous type 1 ECG and an episode of syncope. Nevertheless, the phenotype of this case may change in future, demonstrating clinical features of ARVC/D, such as symptoms of heart failure and RV arrhythmias.

Characteristic clinical features of an overlap disease of BrS and ARVC/D remain unclear, and consensus on a better treatment course for this type of overlap disease remains. After studying the present case, we recommend EPS evaluation to determine the phenotype of overlapping disease (e.g., BrS-like or ARVC/D-like) because clinical features of BrS and those of ARVC/D can coexist in a single patient. The phenotype observed in this case resembled BrS rather than ARVC/D. This case had neither late gadolinium enhancement on CMR nor inducibility of VT/VF during EPS before pilsicainide infusion. Therefore, the existence of scar areas or substrates, which are characteristics of ARVC/D, was unlikely. VF was easily inducible after pilsicainide infusion and was obviously inhibited after ISP infusion. These findings exactly match the characteristics of BrS. Identification of the phenotype of overlapping disease is important because responses to exercises or drugs, such as beta stimulants or sodium channel blockers, differ considerably between BrS and ARVC/D. In addition, upon confirmation of the overlap state, the clinician should recall that the phenotype may change during the clinical course. Therefore, more attentive follow-up is required. As more cases are discovered and reported, this disease state will be expected to be clarified further.

Conflict of interest

No authors in this study report a conflict of interest or need for financial disclosure.

References

[1] Antzelevitch C, Brugada P, Borggrefe M, et al. Brugada syndrome: report of the second consensus conference: endorsed by the Heart Rhythm Society and the European Heart Rhythm Association. Circulation 2005;111:659–70.
[2] Catalano O, Antonaci S, Moro G, et al. Magnetic resonance investigations in Brugada syndrome reveal unexpectedly high rate of structural abnormalities. Eur Heart J 2009;30:2241–8.
[3] Letsas KP, Efremidis M, Weber R, et al. Epsilon-like waves and ventricular conduction abnormalities in subjects with type 1 ECG pattern of Brugada syndrome. Heart Rhythm 2011;8:874–8.
[4] Hoogendijk MG. Diagnostic dilemmas: overlapping features of brugada syndrome and arrhythmogenic right ventricular cardiomyopathy. Front Physiol 2012;3:144.
[5] Peters S, Trümmel M, Denecke S, et al. Results of ajmaline testing in patients with arrhythmogenic right ventricular dysplasia–cardiomyopathy. Int J Cardiol 2004;95:207–10.
[6] Peters S, Trümmel M, Koehler B, et al. QRS fragmentation in standard ECG as a diagnostic marker of arrhythmogenic right ventricular dysplasia–cardiomyopathy. Heart Rhythm 2008;5:1417–21.
[7] Zhang L, Riera ARP, Pu J, et al. Are epsilon waves in ARVD "the right precordial leads only" phenomena? Europace 2006;8(Suppl 1):S265/4.
[8] Papavassiliu T, Wolpert C, Flüchter S, et al. Magnetic resonance imaging findings in patients with Brugada syndrome. J Cardiovasc Electrophysiol 2004;15:1133–8.
[9] Zumhagen S, Spieker T, Rolinck J, et al. Absence of pathognomonic or inflammatory patterns in cardiac biopsies from patients with Brugada syndrome. Circ Arrhythm Electrophysiol 2009;2:16–23.
[10] Koopmann TT, Beekman L, Alders M, et al. Exclusion of multiple candidate genes and large genomic rearrangements in SCN5A in a Dutch Brugada syndrome cohort. Heart Rhythm 2007;4:752–5.
[11] Tada H, Aihara N, Ohe T, et al. Arrhythmogenic right ventricular cardiomyopathy underlies syndrome of right bundle branch block, ST-segment elevation, and sudden death. Am J Cardiol 1998;81:519–22.